Molecular Ecology

WILEY

MOLECULAR ECOLOGY

ORIGINAL ARTICLE OPEN ACCESS

Reduced-Representation Sequencing Detects Trans-Arctic Connectivity and Local Adaptation in Polar Cod (*Boreogadus saida*)

Sarah M. Maes[1,2] | Marie L. Verheye[1] | Caroline Bouchard[3,4] | Enora Geslain[1] | Bart Hellemans[1] | Torild Johansen[5] | Magnus Lucassen[6] | Felix C. Mark[6] | Anna H. Ólafsdóttir[7] | Pauline Snoeijs-Leijonmalm[8] | Daria Zelenina[9] | MOSAiC Team Eco | Filip A. M. Volckaert[1] | Henrik Christiansen[1,10] | Hauke Flores[6]

[1]Laboratory of Biodiversity and Evolutionary Genomics, KU Leuven, Leuven, Belgium | [2]Animal Sciences Unit, Flanders Research Institute for Agriculture, Fisheries and Food, Oostende, Belgium | [3]Greenland Climate Research Centre, Greenland Institute of Natural Resources, Nuuk, Greenland | [4]Department of Biology, Université Laval, Québec, Québec, Canada | [5]Tromsø Department, Norwegian Institute of Marine Research, Tromsø, Norway | [6]Alfred Wegener Institute Helmholtz Center for Polar and Marine Research, Bremerhaven, Germany | [7]Marine and Freshwater Research Institute, Hafnarfjörður, Iceland | [8]Department of Ecology, Environment and Plant Sciences, Stockholm University, Stockholm, Sweden | [9]Department of Molecular Genetics, Russian Federal Institute of Fisheries and Oceanography, Moscow, Russia | [10]Department of Fish and Shellfish, Greenland Institute of Natural Resources, Nuuk, Greenland

Correspondence: Marie L. Verheye (marie.verheye@kuleuven.be)

Received: 22 February 2024 | **Revised:** 30 November 2024 | **Accepted:** 5 December 2024

Handling Editor: J A H Benzie

Funding: This work was made possible by indispensable field support from Fokje Schaafsma, Michiel van Dorssen, Benjamin Lange, Martina Vortkamp, Antonia Immerz, Erik Sulanke, Kim Vane, Elisa Bravo-Rebolledo, Nils Koschnick, Jennifer Steffen, Erin Kunisch, Mai Apasiri Klasmeier, Nadya Zakharova, Ron ten Boer, Franz Mueter, Jared Weems, Alexei Pinchuk, Lorena Edenfield, Kristina Kunz, Nicole Hildebrandt, Anders Svensson, Giulia Castellani, Serdar Sakinan, and Katrin Schmidt. S.M.M. benefited from a fellowship for strategic basic research from the Research Foundation—Flanders (Belgium; grant no. 1S04418N). M.L.V. benefited from postdoctoral funding from EU tender EFICA (contract no. EASME/EMFF/2018/003). H.C. was supported by a fellowship from the former Flemish Agency for Innovation by Science and Technology, now Flanders Innovation and Entrepreneurship (VLAIO, grant 141328). Research of S.M.M., M.L.V., E.G., and H.C. was supported by research infrastructure grant I001621N of EMBRC Belgium—Research Foundation Flanders. The GO-WEST team and expedition were supported by ARICE grant 730965, Bureau of Ocean Energy Management (BOEM) Award #M19AC00018 and the University of Alaska Fairbanks (ship time). Research was funded by the Helmholtz Association Research Programme Polar Regions and Coasts in the changing Earth System II (PACES II), Topic 1, WP 4, and is part of the Helmholtz Association Young Investigators Group *Iceflux*: Ice-ecosystem carbon flux in polar oceans (VH-NG-800) and the EU EFICA project. The SUIT net was developed by Wageningen Marine Research (formerly IMARES) with support from the Netherlands Ministry of Agriculture, Nature and Food Quality (projects WOT-04-009-036 and WOT-04-009-047.04) and the Netherlands Polar Programme (NWO project 866.13.009), which also supported research during RV *Polarstern* expeditions PS80 and PS92. PS122 data used in this manuscript were produced as part of the international Multidisciplinary drifting Observatory for the Study of the Arctic Climate (MOSAiC) with the tag MOSAiC20192020. Work during MOSAiC, PS92 and PS106 was funded by the Dutch Research Council grants 866.18.003 and 866.13.009.

Keywords: Arctic Ocean | fish | Gadidae | polar cod | population genomics | sea ice | seascape | single nucleotide polymorphism

ABSTRACT

Information on connectivity and genetic structure of marine organisms remains sparse in frontier ecosystems such as the Arctic Ocean. Filling these knowledge gaps becomes increasingly urgent, as the Arctic is undergoing rapid physical, ecological and

Sarah M. Maes and Marie L. Verheye joint first authors.

Henrik Christiansen and Hauke Flores joint senior authors.

See details for "MOSAiC Team Eco" in Supporting Information.

[Correction added on 22 March 2025, after first online publication: Ethics Statement section has been updated.]

socio-economic changes. The abundant and widely distributed polar cod (*Boreogadus saida*) is highly adapted to Arctic waters, and its larvae and juveniles live in close association with sea ice. Through a reduced-representation sequencing approach, this study explored the spatial genetic structure of polar cod at a circum-Arctic scale. Genomic variation was partitioned into neutral and adaptive components to respectively investigate genetic connectivity and local adaptation. Based on 922 high-quality single nucleotide polymorphism (SNP) markers genotyped in 611 polar cod, broad-scale differentiation was detected among three groups: (i) Beaufort –Chukchi seas, (ii) all regions connected by the Transpolar Drift, ranging from the Laptev Sea to Iceland, including the European Arctic and (iii) West Greenland. Patterns of neutral genetic structure suggested broadscale oceanographic and sea ice drift features (i.e., Beaufort Gyre and Transpolar Drift) as important drivers of connectivity. Genomic variation at 35 outlier loci indicated adaptive divergence of the West Greenland and the Beaufort–Chukchi Seas populations, possibly driven by environmental conditions. Sea ice decline and changing ocean currents can alter or disrupt connectivity between polar cod from the three genetic groups, potentially undermining their resilience to climate change, even in putative refugia, such as the Central Arctic Ocean and the Arctic Archipelago.

1 | Introduction

Many marine animals are characterised by high fecundity, large population sizes, a pelagic larval phase and extensive geographic ranges, potentially leading to long-distance dispersal of early life stages and adults (Palumbi 2003; Pascual et al. 2017). Such life history traits combined with far-reaching marine currents are expected to result in high gene flow and limited genetic population structuring (Doherty et al. 1995; Schiebelhut and Dawson 2018). Yet other biological (e.g., larval behaviour and local adaptation) and physical processes (e.g., local retention and isolation-by-distance) drive population heterogeneity in marine species (Pineda et al. 2007; Nielsen et al. 2009). Moreover, climate-induced impacts on recruitment, distribution range and disturbances in dispersal pathways through oceanographic alterations likely reshape the genetic structure of species through alterations in connectivity (Andrello et al. 2015; Chan et al. 2018). Genetic connectivity, the exchange of genetic material between individuals from populations (Palumbi 2003), sustains population dynamics as well as genetic variation and adaptive potential and is therefore critical for viability and long-term resilience (Crooks and Sanjayan 2006). Therefore, a baseline understanding of past and present connectivity is conditional to predict how species are affected by climate change and anthropogenic disturbances (Brodersen and Seehausen 2014).

Filling knowledge gaps on connectivity and genetic structure of marine organisms in the rapidly changing Arctic Ocean is vital (Hardy et al. 2011; Geoffroy et al. 2023; Thomas et al. 2022). Over the past 40 years, the Arctic Ocean has experienced a decline in sea-ice extent and a prolonged open-water season (Crawford et al. 2021; Gascard et al. 2019; Kumar et al. 2020). Moreover, ice-free summers are predicted by 2030 (Kim et al. 2023). Climate-driven changes have drastic impacts on marine Arctic ecosystems, including community composition and distribution shifts, changes in abundances, food webs, biogeochemical cycles, and ecosystem services (Lannuzel et al. 2020; Steiner et al. 2021; Wassmann 2011). Sea ice supports entire ecosystems from primary producers such as sea-ice algae to zooplankton, fishes and marine mammals and birds. Its progressive loss results in decreased spatio-temporal availability of a key habitat, used by ice-associated organisms for feeding, reproduction and protection (reviewed by Steiner et al. 2021). Sea ice also serves as a means of dispersal for the associated biota (e.g., Berge et al. 2012; David et al. 2016). The two main currents in the Arctic Ocean, the anticyclonic Beaufort Gyre in the Canada Basin and the Transpolar Drift, flowing from the Siberian shelves over the Central Basin towards Fram Strait, are the main drivers of long-range surface water and ice transport. They play a role in shaping the connectivity patterns of marine organisms, which is reflected in their population genetic diversity and structure (DeHart et al. 2020; Mathiesen et al. 2017). In the last decades, a marked increase in the speed of ice transport by those two wind-driven currents was observed, due to a mechanically weaker, thinning ice cover (Kwok et al. 2013). Increased sea-ice melt, however, may ultimately interrupt these conveyor belts (Krumpen et al. 2019; Kwok et al. 2013; Spreen et al. 2009). Such large-scale changes in circulation patterns and marine habitats will likely disrupt population connectivity of ice-associated organisms across the Arctic Ocean.

Polar cod (also called Arctic cod; *Boreogadus saida* Lepechin, 1774; Gadidae) is a key ice-associated organism distributed across the entire Arctic Ocean, from the shelves to the deep central basins, including the under-ice surface waters (Mueter et al. 2016; David et al. 2016; Snoeijs-Leijonmalm et al. 2021). Adults spawn on the Arctic shelves from late November to March, mostly in January–February (Craig et al. 1982; Graham and Hop 1995; Ponomarenko 2000). The buoyant eggs rise to the ice-water interface where they develop (Laurel et al. 2018; Spencer et al. 2020). Immatures and juveniles are commonly observed in surface waters, beneath the sea ice or in cracks, wedges and cavities within the ice (reviewed by Geoffroy et al. 2023), where they rely on zooplankton and sympagic fauna for prey (Kohlbach et al. 2017). Sea ice likely serves as a transport vector for the early life stages through long-distance ice drift (David et al. 2016; Maes et al. 2021), before they transition to deeper and warmer Atlantic water, joining larger conspecifics (Geoffroy et al. 2011). Adults may undertake spawning and feeding migrations of up to about 200 km (Aune et al. 2021; Ponomarenko 1968; Kessel et al. 2017). Polar cod is the most abundant forage fish in the Arctic Ocean and may be found in very dense shoals (Melnikov and Chernova 2013; Welch et al. 1992). It transfers most of the energy from lower trophic levels such as zooplankton to higher trophic levels, such as piscivorous fishes, marine mammals and seabirds (Bradstreet and Cross 1982; Kohlbach et al. 2017) and is locally harvested as bait (Bouchard et al. 2023). However, ocean

warming and loss of under-ice habitat may compromise its survival and recruitment in some regions. Decreased abundance and a northward range shift of polar cod might lead to cascading impacts on higher trophic levels (Geoffroy et al. 2023; Steiner et al. 2021).

The life-history characteristics of polar cod might lead to weak population structuring due to their high dispersal capacity, both at the larval and adult stages. Initial studies based on mitochondrial DNA and microsatellite markers found little to no genetic structure across wide areas of the Arctic Ocean, such as from Baffin Bay and the Greenland Sea (Pálsson et al. 2009) to the Barents Sea (Fevolden and Christiansen 1997), Svalbard fjords and the Central Arctic Eurasian basins (Maes et al. 2021), and from the Chukchi and Beaufort seas (Wildes et al. 2016; Wilson et al. 2019) to the Bering Sea (Wilson et al. 2020). Similarly, no spatial population structure was detected between Svalbard and the Kara Sea using single nucleotide polymorphisms (SNPs; Quintela et al. 2021), whereas small but significant differentiation was found on the Russian shelves (between the Laptev and East Siberian seas; Quintela et al. 2021; Gordeeva and Mishin 2019). Microsatellite markers showed differentiation between neighbouring fjord and offshore sites along northeast Greenland and West Svalbard (Madsen et al. 2016). The potential presence of two ecotypes (i.e., coastal and oceanic type), which have also been suggested based on morphological features in the Russian Arctic (Chernova et al. 2021; Moskalenko 1964), implies that local adaptation may play an important structuring role (Madsen et al. 2016). To date, two studies have explored the population structure of polar cod at a large scale, albeit without samples from the Central Arctic Ocean (CAO). In the first study based on microsatellite markers, four genetic groups were identified: (i) the Siberian shelves to Fram Strait and Iceland, (ii) the eastern coastline of Canada from Resolute Bay to the Gulf of St. Lawrence, (iii) the Canadian coast of the Beaufort Sea and (iv) the Alaskan Beaufort and Chukchi seas (Nelson et al. 2020). A second study using SNP markers and focusing on the Canadian coastlines confirms differentiation between the Beaufort Sea and Baffin Bay, whereas Hudson Bay, the subarctic waters of the Newfoundland and Labrador shelves, and the Gulf of St. Lawrence are also differentiated from the higher Arctic locations (Bringloe et al. 2024). Moreover, three recent studies reveal chromosomal inversion patterns without obvious spatial structure; their adaptive role remains unexplored (Bringloe et al. 2024; Einarsson et al. 2023; Hoff, Maurstad, Le Moan, et al. 2024).

Hence, high-resolution genomic data are a powerful tool to reveal fine-scale genetic structure (Gagnaire 2020). In addition, sampling hundreds of genetic markers across the genome allows discrimination between genome-wide (i.e., drift and migration) and locus-specific (i.e., selection) effects (Nielsen et al. 2009; Stinchcombe and Hoekstra 2008). Genomic approaches therefore disentangle population connectivity and adaptive divergence, together shaping the spatial population structure (Crawford and Oleksiak 2016). For the first time, we use a genomic approach to explore the population structure of polar cod at a circumpolar scale. Using reduced representation sequencing, we aim to (i) improve the resolution of spatial genetic structure patterns within and among Arctic ecoregions, (ii) explore neutral genetic structure to understand genetic connectivity between populations across the entire Arctic Ocean and (iii) investigate the influence of spatial and environmental variation on adaptive divergence to uncover evidence of local adaptation. Sound knowledge of connectivity and adaptation patterns will help understand how this key Arctic marine species may cope with rapid environmental shifts.

2 | Materials and Methods

2.1 | Sample Collection

A total of 652 polar cod samples were collected in the Central Arctic Ocean, Fram Strait and the Arctic Ocean shelves bordering Alaska, Canada, Russia, Greenland, and Northern Europe during several expeditions between 2003 and 2021 (Figure 1; Appendix S1). Fish were collected using bottom trawl, bongo net, Young fish trawl (Methot 1986), Surface and Under-Ice Trawl, ROVnet, Multpelt 832 pelagic trawl (ICES 2013a, 2013b), or zooplankton net. Juvenile fish were identified morphologically by experts onboard. Larvae were identified using DNA barcoding of the mitochondrial COI gene, following the protocol described in Bouchard et al. (2021) for molecular specimen identification. We collected fin clips of all fish sampled and stored them in 96% ethanol.

Given the constraints of sampling in remote and ice-covered areas, only a few (< 10) individuals were collected at some sites. In order to establish biologically sound groupings of sampling sites into putative populations, as a basis for further population genetic analyses, we relied on the Marine Ecoregions of the World (MEOW; Spalding et al. 2007). For the Arctic Ocean, 19 ecoregions have been established, which are defined as areas of relatively homogeneous species composition, clearly distinct from adjacent regions. The dominant biogeographic forcing agents may include isolation, upwelling, nutrient inputs, freshwater influx, temperature regimes, ice regimes, exposure, sediments, currents, and bathymetric or coastal complexity (Spalding et al. 2007). Samples cover seven ecoregions (North and East Iceland, West Greenland shelf, High Arctic Archipelago, Beaufort Sea–continental coast and shelf, Chukchi Sea, Laptev Sea, and North and East Barents Sea; Figure 1). As MEOW includes only a classification of shelf and coastal areas, two additional offshore ecoregions were defined: Fram Strait and High Arctic. These belong to distinct large marine ecosystems (LME), that is, East Greenland shelf–Sea and Arctic Ocean, respectively (Hempel and Sherman 2003; Sherman et al. 2005; Siron et al. 2008).

In the High Arctic and North and East Barents Sea ecoregions, sampling sites were spread over a wide geographical area and sometimes characterised by distinct environmental conditions. For instance, oceanographic and environmental conditions across the Svalbard archipelago range from strongly Atlantic-influenced waters on the west coast to high-Arctic conditions in northeast Svalbard (Cottier et al. 2010). Therefore, we defined further spatial subdivisions within the latter two ecoregions to test for genetic differentiation. In the High Arctic ecoregion, sampling sites were grouped into locations according to ocean basin (Amundsen and Nansen Basins). In the North and East Barents Sea ecoregion, sampling

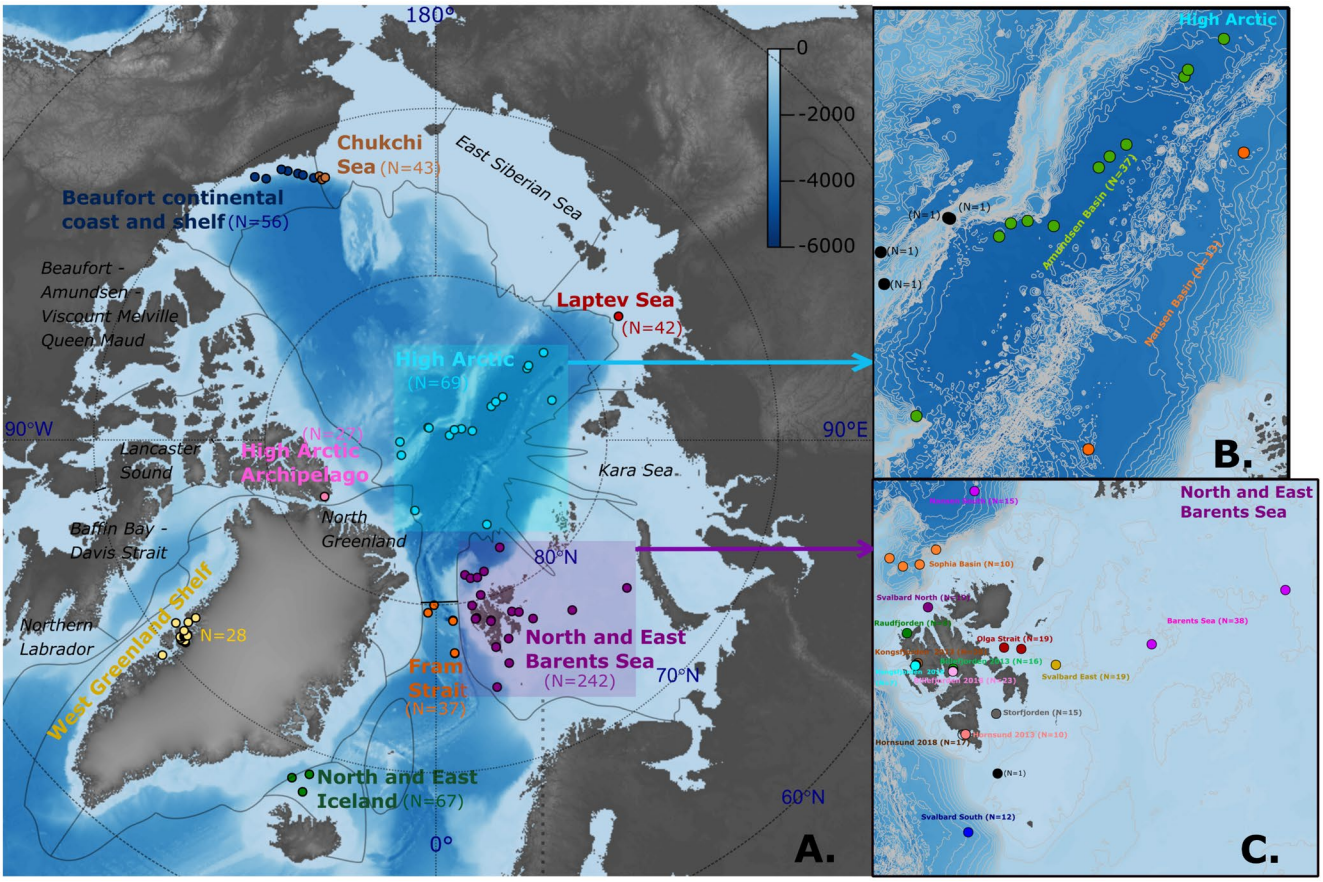

FIGURE 1 | Map of the Arctic Ocean showing the sampling sites. (A) Sampling sites are coloured according to ecoregions *sensu* Spalding et al. (2007). (B) Zoom on the sampling sites in the High Arctic ecoregion; light grey lines are 200 m isobaths and sites are coloured according to basin (Amundsen and Nansen Basins). (C) Zoom on the sampling sites in the North and East Barents Sea ecoregion; light grey lines are 200 m isobaths and sites are coloured according to location and sampling year. To produce these maps, the International Bathymetric Chart of the Arctic Ocean (IBCAO) was downloaded from the General Bathymetric Chart of the Oceans (GEBCO) website (https://www.gebco.net) in netCDF format, 400 m × 400 m grid cell spacing and including elevation data for the Greenland Ice Sheet.

sites were grouped according to fjord system, sampling year, archipelago location (North, South and East Svalbard) and depth (Figure 1).

2.2 | DNA Extraction and Sequencing

Genomic DNA was extracted from fin clips using the NucleoSpin Tissue kit (Macherey-Nagel), following the manufacturer's instructions. A modified version of the Elshire et al. (2011) genotyping-by-sequencing (GBS) method was used, with a single restriction enzyme (*PstI*) and size selection (320–720 bp). Genomic DNA (100 ng; 10 ng/μL) was fragmented by a master mix containing 1 μL *PstI* (20 U^2), 2 μL 10× NEB buffer (NEB), 1 μL H_2O and 6 μL of unique barcode adapter mix (20 nM) per sample, followed by subsequent incubation at 37°C for 2 h. For ligation, a master mix containing 5 μL 10× NEB DNA ligase buffer, 1.2 μL T4 ligase (400 U/μl) and 23.8 μL H_2O per sample and 20 μL DNA was incubated for 1 h at 22°C followed by 30 min at 65°C and purified using CleanPCR beads. The purified ligation product (1 μL) was amplified in a PCR containing 12.5 μL NEB Q5 hotstart master mix (NEB), 10.5 μL H_2O, and 1 μL forward and reverse primer (both 5 μM). The PCR thermal cycling steps started with an initial denaturation step of 30 s at 98°C, followed by 18 cycles of 10 s at 98°C, 30 s of annealing at 65°C, 30 s of extension at 72°C, and ending with a final extension of 5 min at 72°C. PCR amplicons were cleaned using CleanPCR beads (CleanNA, GC Biotech) and quantified using the Quant-iT Picogreen kit (ThermoFisher Scientific). PCR products with at least 10 ng DNA were pooled. Four GBS libraries were paired-end sequenced on an Illumina Novaseq platform 6000 (PE100) at the Genomics Core Leuven (www.genomicscore.be).

2.3 | Bioinformatics

Sequences were quality checked using FastQC v0.11.8 (Andrews 2010). Stacks v2.5 was used to process the GBS data (Catchen et al. 2013; Rochette et al. 2019). First, raw sequence reads were demultiplexed and trimmed using the process_radtags module (with parameters -r, -q). Subsequently, reads were aligned to a draft *Boreogadus saida* reference genome (GenBank accession number GCA_900302515.1) using Bowtie2 v2.3.4.3 (Langmead and Salzberg 2012). A total of 37 individuals with < 1,000,000 reads, < 15× or > 150× coverage, and/or < 60 mapping success were removed (Appendix S2). SNPs were called using default parameters in Stacks, which employs a Bayesian genotype caller (Maruki and Lynch 2017). Only SNPs genotyped

in at least 70% of the individuals within each sampling site, a maximum heterozygosity of 0.70 and an overall minor allele frequency (MAF) of > 0.05 were retained. Further SNP filtering was done using VCFtools v.0.1.16 (Danecek et al. 2011) with the following criteria: no loci and individuals with more than 20% missing data, an overall minor allele frequency (MAF) of > 0.05, and a minimum minor allele count of 5. The SNP dataset was pruned to be in approximate linkage disequilibrium using the R function snpgdsLDpruning from R package *SNPRelate* v1.28.0 (Zheng et al. 2012), with an ld.threshold of 0.2 and removing monomorphic loci. As a Principal Component Analysis (PCA) of the resulting data set revealed a library bias, the SNPs driving this batch effect were excluded, following the procedure detailed in marineomics.github.io (Bogan et al. 2023; Silliman and Davenport 2022. The PC loadings were first extracted for each SNP for the PC that represents the batch effect. Loci with the largest effect (high PC loadings) were removed until no library effect was detectable anymore. PCAs and loadings are reported in Appendix S3. Furthermore, loci with more than 20% missing data and/or heterozygosity > 0.6, and individuals with more than 30% missing data were filtered out using R packages *poppr* v.2.9.3 (Kamvar et al. 2014) and *hierfstat* v.0.5–11 (Goudet 2005). Finally, departures from Hardy–Weinberg proportions (HWP) were tested per locus per station with R package *pegas* v1.1 (Paradis 2010), after correcting for multiple testing using a threshold q-value of 0.05 with R package *qvalue* v2.26.0 (Dabney et al. 2010). Loci that were not in HWP in any population were removed.

2.4 | Summary Statistics and Population Differentiation

Standard indices of genetic diversity, that is, observed and expected heterozygosity (H_o and H_e) and inbreeding coefficient (F_{IS}), were calculated for each putative population using the function *basic.stats* (R package *hierfstat* v.0.5–11). Genetic differentiation between putative populations was estimated with pairwise F_{ST} values (Weir and Cockerham 1984). Respective *p*-values were assessed after performing 1000 permutations over individuals across populations, using a *p*-threshold of 0.05 and Benjamini-Hochberg correction for multiple tests. Genetic distances were visualised with classical multidimensional scaling (MDS) of F_{ST} values using the *cmdscale* function (R package stats v.3.6.2.).

2.5 | Detection of Putatively Adaptive Loci

First, we conducted population genetic analyses with the total data set of 922 SNPs (see Section 2.6). Then, we identified putatively adaptive loci based on the 1192 SNPs data set (unfiltered for HWE) and repeated the population genetic analyses using putatively neutral and putatively adaptive SNP subsets.

Three different methods were used to identify candidate loci under natural selection. To decrease the likelihood of selecting false positives, a SNP was considered putatively adaptive when it was identified as an outlier by at least two of these methods. Firstly, BayeScan is a Bayesian method that estimates the posterior probability of SNP markers being under selection based on two alternative multinomial Dirichlet models, including selection or not. Selection is introduced by decomposing F_{ST} coefficients into a population-specific component shared by all loci and a locus-specific component shared by all the populations. Departure from neutrality at a given locus is assumed when the locus-specific component is necessary to explain the observed pattern of diversity (Beaumont and Balding 2004; Foll and Gaggiotti 2008). BayeScan v2.1 was run for 10,000 iterations and a burn-in of 200,000 steps. The prior odds of neutrality parameter was set to 10,000 following Lotterhos and Whitlock (2014). The false discovery rate q-value threshold was set to 0.01. Secondly, OutFLANK estimates the null distribution of F_{ST} by trimming loci with the highest and lowest F_{ST} values from the empirical distribution, assuming that the majority of loci in the centre of the distribution are neutral. The full untrimmed distribution of F_{ST} is estimated based on the best-fitting χ^2 distribution, conditioned on the values observed within the two trimming bounds. Loci that are unusual relative to this inferred distribution may be experiencing strong spatially heterogeneous selection (Whitlock and Lotterhos 2015). OutFLANK v0.2 was run using the following parameters: left and right trim of 0.05, minimum heterozygosity of 0.1, and qvalue threshold of 0.01. Lastly, we used an individual-based method, PCAdapt, which assumes that candidate markers are outlier loci concerning how they are related to population structure as represented by a PCA. Mahalanobis distances between the correlations of each SNP with the principal components and the mean correlations are computed. The distribution of those distances scaled by a constant is expected to have a chi-squared distribution with *K* degrees of freedom under the assumption that there are no outlier loci. Individual SNPs significantly departing from this null distribution, using q-values to correct for the false discovery rate, are detected as outlier loci. The latter method was applied using R packages *PCAdapt* v4.1.0 and *qvalue* v2.14.1 with q-threshold of 0.01 (Dabney et al. 2010; Luu et al. 2017).

2.6 | Population Structure

Principal component analyses (PCA) were performed using the function *dudi.pca* (R package *ade4* v.1.7.19). The PCA reduces the data to a smaller number of dimensions termed principal components (PCs), while preserving their covariance. Each PC describes a decreased proportion of the genomic variation, and genotypes are then projected onto the space spanned by the PC axes. A Discriminant Analysis of Principal Components (DAPC) was computed using the R package *adegenet* v.2.1.8 (Jombart and Ahmed 2011). In the DAPC, the genotype data set is transformed using PCA to derive uncorrelated variables that serve as input for discriminant analysis (DA). The DA aims to maximise among-group variation and minimise within-group variation (Jombart et al. 2010; Miller et al. 2020). A first DAPC was used to visualise a priori defined geographical groupings, that is, ecoregions. A second DAPC was performed without defining populations a priori. Instead, successive *K*-means clustering performed on PCA-transformed data was used to define clusters using the R function *find.clusters*. The most likely *K* was selected based on the Bayesian Information Criterion (BIC). The number of PCs to retain for both DAPCs was determined using *a*-score optimization to avoid overfitting, using the function *optim.a.score* (Jombart et al. 2010).

Clustering analysis with STRUCTURE v2.3.4 (Pritchard et al. 2000) was performed with 100,000 burn-ins, 100,000 MCMC repeats, an admixture model, and 10 iterations for each *K* from 1 to 10. The StructureSelector Web Server (https://lmme.ac.cn/StructureSelector/) was used to visualise the output and to assess the most likely number of clusters (Li and Liu 2018), using both the four new supervised estimators MEDMEDK, MEDMEAK, MAXMEDK, and MAXMEAK from Puechmaille (2016) and the Delta *K* method of Evanno et al. (2005). The 10 runs of STRUCTURE for the most probable *K* were averaged using CLUMPP v 1.1.2 (Jakobsson and Rosenberg 2007), and the results were then graphically displayed in Excel.

2.7 | Spatial Structure and Environmental Variables

In-water distances (i.e., shortest distance through water deeper than 0.1 m) were computed based on the geographical coordinates of the 46 sites using the *lc.dist* (R package *marmap* v.1.0.6) function (Pante and Simon-Bouhet 2013) in R and the bathymetric map of the Arctic Ocean ('IBCAO') downloaded from GEBCO (https://www.gebco.net) (Jakobsson et al. 2020). Spatial structure was then modelled using distance-based Moran's eigenvector map (dbMEMs) variables using the *dbmem* function (R package *adespatial* v.0.3–20). dbMEMs are independent vectors that summarise the geographic distances among sampling sites (Borcard and Legendre 2002).

We employed a set of 16 climate and biogeochemical variables, as potential drivers of genomic variation in polar cod, to characterise the seascape. We obtained these variables from a georeferenced dataset describing seawater conditions from the Copernicus Marine Environment Monitoring Service (CMEMS: https://marine.copernicus.eu/). This data set (product ARCTIC_MULTIYEAR_PHY_002_003) includes the following oceanographic variables as monthly mean values with a 12.5 km resolution for the period 1991–2021: sea surface temperature ('SST';°C), sea surface salinity ('SSS'; [10–3]), mixed layer thickness (MLT; m), surface sea current and sea ice velocity ('SCV' and 'SICV'; m/s), sea ice area fraction ('SIA'; %) and sea ice thickness ('SIT'; m).

These variables were imported in R as stacks of monthly raster layers to compute the overall means and standard deviations and retrieve the values for each of the sampling sites. For ice-related variables (SIA and SIT), the maximum summer and winter values were calculated as well as the overall standard deviation.

2.8 | Redundancy Analyses

We conducted redundancy analyses (RDA) to investigate the correlation between neutral and putatively adaptive genetic variation and a set of environmental variables at an ecoregional scale, using the R package *vegan* v.2.6–2. RDA is a direct extension of multiple regression to model multivariate response data (Legendre and Gallagher 2001). Allelic frequencies were computed for the 922 loci in each population. The populations were generally defined as sampling sites. However, at some sites, only one or very few specimens were collected. These sites were either removed or grouped with neighbouring sites, resulting in a total of 41 locations (see Appendix S4 for details). A detrending of the raw allelic frequency data was applied using the *decostand* function with the Hellinger method (Oksanen et al. 2007). Next, we performed a principal component analysis (PCA) of the allelic frequency data and only retained the principal component factors (PCs) with eigenvalues greater than the mean eigenvalue, according to the Kaiser–Guttman criterion (Yeomans and Golder 1982). The latter PCs were used as response variables in the RDA. To limit multicollinearity among the environmental variables, we calculated their variance inflation factor (VIF) using the *vif.cca* function and successively deleted variables with the highest VIF until all VIFs were below 20. Then, an automatic stepwise model-building procedure was performed using the *ordistep* function in both directions, which iteratively adds or removes variables in order to build a model that maximises the adjusted R^2. The selected dbMEM and environmental variables were used as explanatory variables in the RDA. Full RDA models were first constructed using the *rda* function and all selected spatial and environmental variables as explanatory variables for the outlier dataset. Then, variance partitioning was performed using the *varpart* function to explore the separate and joint contributions of the spatial (dbMEM) and environmental variables in explaining the putatively adaptive genetic variation. In all RDA tests, analyses of variance (ANOVAs; 1000 permutations) were performed to assess the global significance of the model and of each RDA axis. The adjusted R^2 was quantified using the *RsquareAdj* function.

3 | Results

3.1 | Reduced-representation Sequencing and SNP Genotyping

On average, 4,531,650 reads per individual were obtained (minimum–maximum: 74–17,625,964). Mean per-sample coverage was 65.7× (minimum–maximum: 4.3–182.5×). Average mapping percentage was 75.2% (minimum–maximum: 0.73%–78.92%; see Appendix S2). A total of 1,599,856 SNPs were called, resulting in 187,756 variants after filtering with Stacks. A summary of the filtering procedure and the number of SNPs removed at each step can be found in Appendix S5. The final data set contained genotypes from 611 individuals across 922 high-quality SNPs.

3.2 | Outlier SNPs

BayeScan identified 18 loci putatively under divergent selection and none under balancing selection. OutFLANK identified 34 loci putatively under divergent selection as well, 15 of which were in common with BayeScan. Finally, PCAdapt detected 90 putatively adaptive loci, 16 in common with BayeScan and 32 with OutFLANK. Fourteen SNPs were common between all three methods. The 35 candidate SNPs identified as putatively adaptive loci by at least two of the methods were used for downstream analyses of adaptive genetic structure. Diagnostic plots for the three outlier detection methods are reported in Appendix S6.

3.3 | Summary Statistics and Population Differentiation

Summary statistics across the total data set of 922 loci for each ecoregion/subregion are shown in Table 1. Observed (H_o) and expected heterozygosity (H_e) ranged from 0.15 to 0.19 and 0.20 to 0.33, respectively (Table 1). F_{IS} values ranged from 0.08 to 0.22.

Pairwise fixation index (F_{ST}) values between the 24 putative populations of polar cod ranged from 0 to 0.05 (between the West Greenland and Beaufort Sea ecoregions) (Figure 2A).

TABLE 1 | Summary statistics of polar cod by ecoregion (shaded) and location: Observed heterozygosity, *Ho*, expected heterozygosity, *He*, and inbreeding coefficient, F_{IS}.

Ecoregion/location	No. ind.	H_o	H_e	F_{IS}
Beaufort continental coast and shelf	56	0.19	0.22	0.14
Chukchi Sea	43	0.19	0.22	0.13
Laptev Sea	42	0.18	0.21	0.14
High Arctic	69	0.18	0.21	0.16
Amundsen Basin	37	0.18	0.21	0.14
Nansen Basin	13	0.18	0.20	0.11
High Arctic Archipelago	27	0.19	0.21	0.11
West Greenland shelf	28	0.18	0.20	0.14
Fram Strait	37	0.17	0.21	0.18
North and East Iceland	67	0.19	0.21	0.11
North and East Barents Sea	242	0.18	0.21	0.15
Nansen South	15	0.17	0.21	0.16
Sophia Basin	10	0.17	0.21	0.15
Svalbard North	19	0.18	0.20	0.10
Raudfjorden	8	0.17	0.20	0.12
Kongsfjorden 2013	29	0.18	0.21	0.12
Kongsfjorden 2018	7	0.18	0.21	0.08
Billefjorden 2013	16	0.18	0.21	0.11
Billefjorden 2018	23	0.19	0.21	0.10
Hornsund 2013	10	0.17	0.21	0.13
Hornsund 2018	17	0.19	0.21	0.09
Storfjorden	15	0.15	0.21	0.22
Svalbard South	12	0.19	0.21	0.10
Olga Strait	19	0.18	0.21	0.12
Svalbard East	19	0.19	0.21	0.08
Barents Sea	38	0.18	0.20	0.10

Note: The sampling sites included in the ecoregions are available in the Appendix S1.

Pairwise F_{ST} values between West Greenland and all other populations were the highest and all significant (mean F_{ST}: 0.038). The Beaufort Sea and Chukchi Sea populations were not differentiated from each other, but were significantly differentiated from all other populations (overall mean F_{ST}: 0.02). Pairwise F_{ST} values among populations from the remaining six ecoregions (High Arctic Archipelago, Laptev Sea, High Arctic, Fram Strait, North and East Iceland, North and East Barents Sea) ranged from 0 to 0.017. Within the High Arctic ecoregion, the Amundsen and Nansen basin populations were not significantly differentiated.

The Multidimensional Scaling (MDS) plot shows the differentiation between West Greenland and other regions mainly on the x-axis, while Beaufort/Chukchi Seas separate from all others on both the x- and y-axes (Figure 2B). The remaining six ecoregions (Laptev Sea, High Arctic, Fram Strait, Iceland, North and East Barents Sea, High Arctic archipelago) cluster together in those two first dimensions; the Laptev Sea shows some differentiation from all others. On the z-axis, the Svalbard East and Barents Sea localities separate from other areas of the North and East Barents Sea, Fram Strait, and Iceland, as being located on the negative side of this third axis.

3.4 | Population Genetic Analyses

3.4.1 | Total Data set

Principal component analysis performed on the total 922 SNPs data set revealed a clear distinction between samples from the 'Beaufort-Chukchi' seas and those from all other ecoregions along PC1 (Figure 3A). Although there is considerable overlap between samples from West Greenland and other ecoregions, the former partially separates from others along both PC1 and PC2 axes. Samples from all remaining ecoregions (Laptev Sea, High Arctic, High Arctic Archipelago, North and East Barents Sea and Iceland) show considerable overlap.

The Bayesian approach of STRUCTURE applied to this total data set suggested three and four genetic groups with Puechmaille (2016)'s estimators and two following Evanno et al. (2005)'s method (Appendix S7). The inferred population membership coefficients for $K=2$ and $K=3$ are shown in Figure 3A. The first cluster (yellow) is dominant in the Beaufort–Chukchi Seas. The yellow cluster is also present in other regions, especially the Laptev Sea, although in lesser proportions. Samples from all regions influenced by the Transpolar Drift Current, from the Laptev Sea to Iceland, passing by the Central Arctic Ocean and Fram Strait and including the European sector of the Arctic Ocean, mainly belong to the second cluster (blue). In the $K=3$ STRUCTURE plot, the third cluster (green) is dominant in West Greenland. A few individuals from all other regions—especially in the High Arctic Archipelago, the Beaufort and Chukchi Seas—also show a major green cluster component. The STRUCTURE plot for $K=4$ did not provide any additional information (Appendix S8A).

The STRUCTURE analysis performed on the High Arctic, Fram Strait, Iceland, and North and East Barents Sea ecoregions suggested one and two genetic groups with

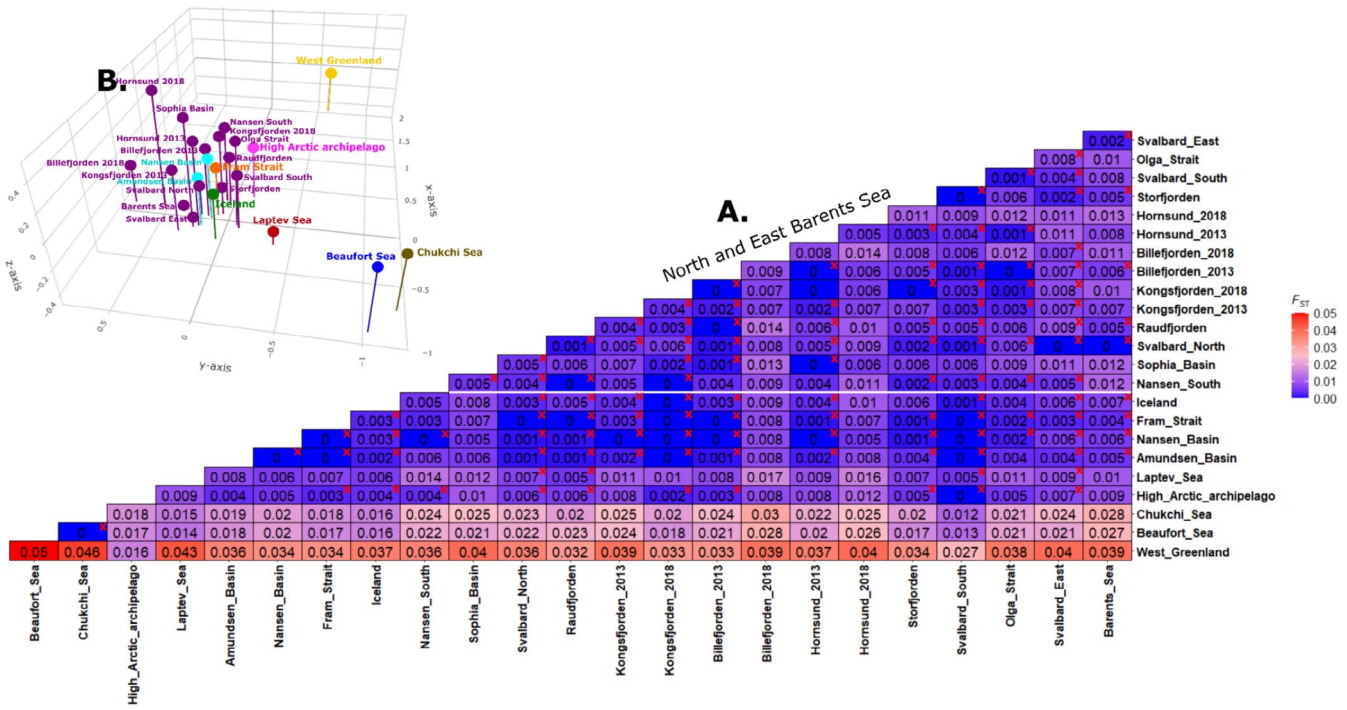

FIGURE 2 | Below: Heatmap representing pairwise F_{ST} values among populations. Red asterisks indicate F_{ST} values not significantly different from zero as revealed by a permutation test (p-threshold: 0.05). Above: Classical multidimensional scaling plot of the pairwise F_{ST} genetic distances with points coloured according to ecoregions.

Puechmaille (2016)'s estimators and two following Evanno et al. (2005)'s method. The inferred population membership coefficients for $K=2$ are shown in Figure 3A. No differences are observed among those ecoregions, which all belong to both (yellow and blue) clusters, with a general dominance of the blue cluster (Figure 3A).

Similar large-scale patterns were observed using Discriminant Analysis of Principal Components (DAPC) with a priori defined populations, namely minimal overlap between the Beaufort-Chukchi groups and all others, as well as West Greenland and all others. The High Arctic Archipelago group has an intermediate position between the West Greenland group on the one hand and, on the other hand, five ecoregional groups, which are largely overlapping, including the Laptev Sea, Iceland, the Central Arctic Ocean, Fram Strait, and the European sector of the Arctic Ocean (Figure 4A). To explore the population structure among the latter five groups in greater detail, another DAPC was performed after excluding the Beaufort-Chukchi, West Greenland, and High Arctic Archipelago clusters. Extensive overlap between the High Arctic, Fram Strait, and North and East Barents Sea groups is apparent, whereas the two geographically most distant samples (Laptev Sea and Iceland) are somewhat distinct (Figure 4B). Using K-means clustering to define clusters for the DAPC with no a priori groupings, $K=2$–4 had minimal (<2) difference in BIC (Appendix S9A). The DAPC performed with $K=2$ shows the distinction of the Beaufort-Chukchi Seas with all other ecoregions (Appendix S9B). The DAPC performed with $K=3$ shows the distinction of the Beaufort-Chukchi Seas as well as two additional clusters with no geographical structure (Appendix S9C). The DAPC performed with $K=4$ additionally shows the distinction of West Greenland to all other ecoregions (Appendix S9D).

3.4.2 | Neutral and Adaptive Population Structure

Using outlier detection results, we decomposed the total data set into its putatively neutral and adaptive components. When considering only loci that are likely not affected by ongoing selection processes ('neutral'—all SNPs detected as putatively adaptive by any method removed), the distinction between samples from the 'Beaufort-Chukchi' seas and, to a lesser extent, the Laptev Sea, and all others remains, albeit much less pronounced compared to the full data set (Figure 3B). In contrast, the separation of West Greenland is minimal in the neutral data set. Correspondingly, STRUCTURE applied to the neutral data set suggested two and three genetic groups with Puechmaille (2016)'s estimators and two following Evanno et al. (2005)'s method (Appendix S7). The inferred population membership coefficients for $K=2$ are shown in Figure 3B. The first cluster (yellow) is dominant in the Beaufort–Chukchi and Laptev Seas, while individuals from other ecoregions show similar ancestry proportions to both (yellow and blue) clusters (Figure 3B). West Greenland individuals do not form a separate cluster. The structure plot for $K=3$ did not provide any additional information (Appendix S8B).

On the PCA based on the 35 putatively adaptive SNPs (identified by at least two outlier detection methods), the 'Beaufort-Chukchi' seas are again recovered as partially distinct (Figure 3C). The separation of the West Greenland sample from the Beaufort-Chukchi and the transpolar drift ecoregions along PC2 is almost complete, with minimal overlap. The High Arctic Archipelago samples have an intermediate position on the PCA biplot, showing partial overlap with West Greenland and all remaining ecoregions. Applying STRUCTURE on this putatively adaptive dataset suggested three and four genetic groups using Puechmaille (2016)'s

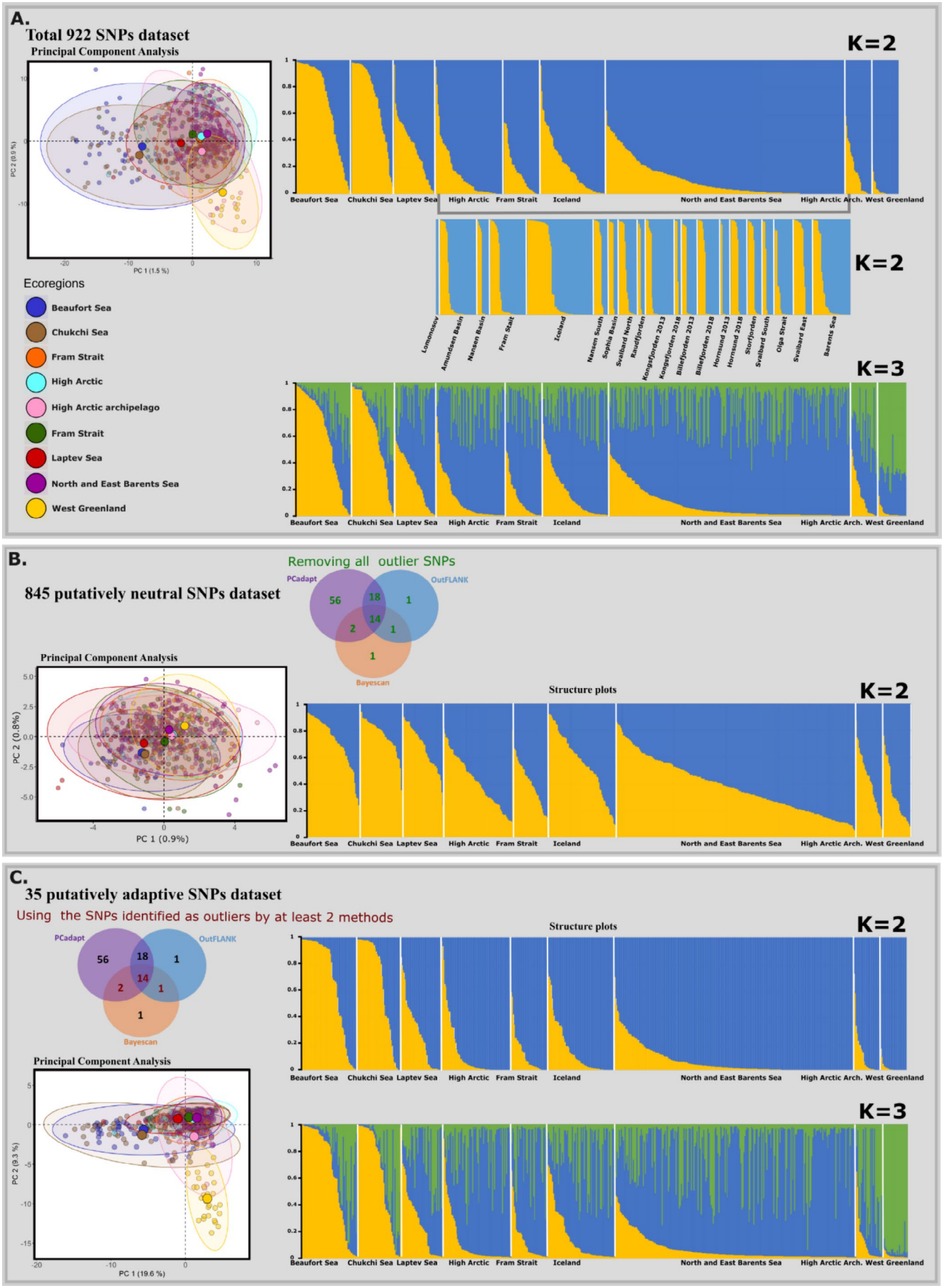

FIGURE 3 | Legend on next page.

FIGURE 3 | Principal component analysis (PCA) with corresponding STRUCTURE plots based on (A) the total 922 SNPs data set, (B) the 845 putatively neutral SNPs and (C) the 35 SNPs identified as putatively adaptive by at least two methods (see Venn Diagram). In the PCAs, dots represent individuals, coloured according to ecoregions. In the STRUCTURE plots, each vertical bar represents an individual, coloured according to the ancestry coefficients (to the *K* clusters).

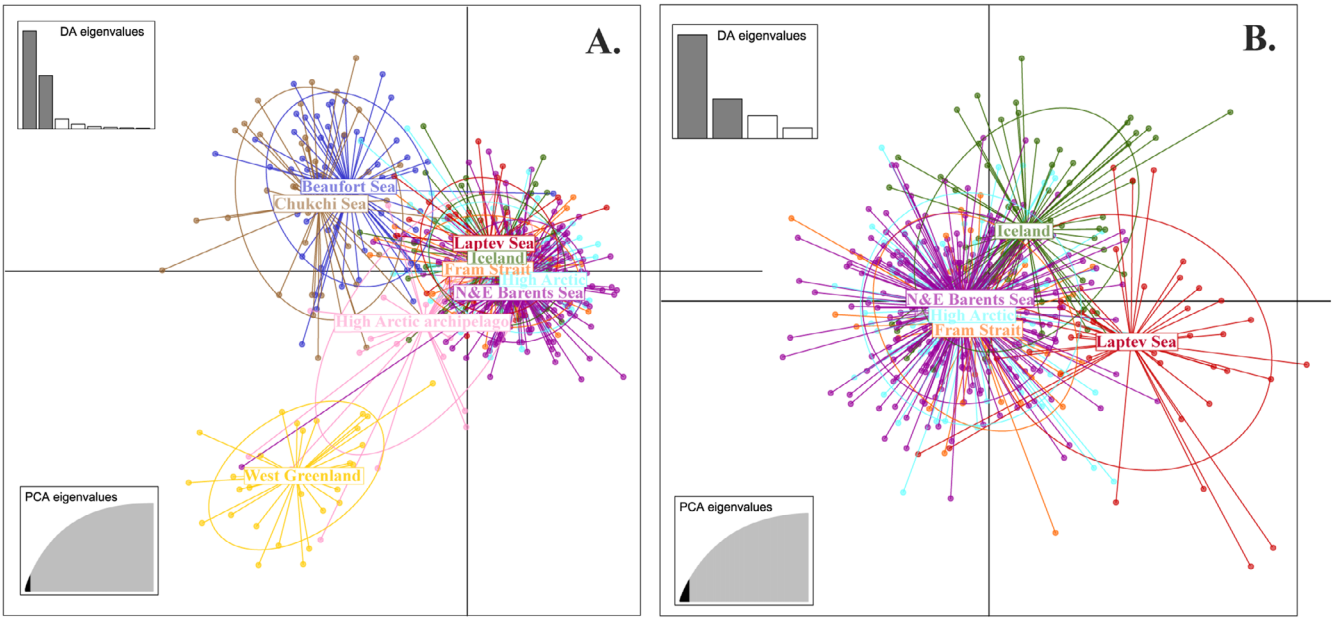

FIGURE 4 | Plots of discriminant analysis of principal components (DAPC) among groups defined by ecoregion and based on 922 SNPs. Inertial ellipses are represented for each group, and each dot represents an individual. The axes represent the first two linear discriminants (LD). (A) DAPC including samples from all nine ecoregions and (B) DAPC including samples from five ecoregions (excluding Beaufort-Chukchi seas, High Arctic archipelago, and West Greenland ecoregions).

estimators and two following Evanno et al. (2005)'s method (Appendix S7). The inferred population membership coefficients for $K=2$ and $K=3$ are shown in Figure 3C. On the $K=2$ STRUCTURE plot, the Beaufort-Chukchi Seas show a major yellow component, while all other ecoregions show a major blue component. On the $K=3$ STRUCTURE plot, individuals from West Greenland belong to a third (green) cluster, which is also dominant in most of the High Arctic Archipelago individuals, some individuals from the Beaufort-Chukchi seas, and is also present in smaller proportions in all other ecoregions. The STRUCTURE plot for $K=4$ did not provide any additional information (Appendix S8C).

Lastly, a distinct pattern emerged when performing a PCA on the 56 SNPs identified by PCAdapt only. Unlike with outlier SNP data sets based on the other detection methods, the PCAdapt outliers revealed three groups separated on both PC1 and PC2, showing a band-like pattern and no geographical structure (Appendix S10).

3.5 | Redundancy Analysis

Using the putatively neutral data set (845 SNPs detected by at least two methods), automatic stepwise model building in both directions of the dbMEM variables resulted in the selection of one dbMEM vector (MEM1). After iteratively excluding environmental variables associated with the highest VIF values until all variables presented a VIF < 20, 10 variables remained: SST_OM (8.23), SST_OSD (18.59), SSS_OM (9.44), SSS_OSD (3.90), SIA_WM (12.46), SIA_OSD (13.72), SIT_SM (12.06), SIT_OSD (15.24), SICV_OM (2.73), and MLT_OSD (2.35). Model building using this set of 10 environmental variables in both directions resulted in the selection of three variables: the winter mean in sea ice area fraction (SIA_WM), the overall standard deviation in sea ice thickness (SIT_OSD) and the overall mean in sea surface salinity (SSS_OM).

The global RDA using the putatively neutral dataset and all selected explanatory variables (MEM1, SIA_WM, SIT_OSD, SSS_OM) was significant (p-value = 0.001) and accounted for 8% of the genomic variation (adjusted $R^2 = 0.08$). Of this total explained variation, 5% was attributable to spatial variables (MEM1), and the remaining proportion (3%) is a joint effect of MEM1 and environmental variables. The first two RDA axes were not significant (p-values = 0.064 and 0.096). Beaufort and Chukchi Sea populations are positively correlated with SIA_WM, SIT_OSD, and MEM1 and negatively with SSS_OM (Appendix S10).

Using the putatively adaptive data set (35 SNPs detected by at least two methods), automatic stepwise model building in both directions of the dbMEM variables resulted in the selection of four dbMEM vectors (MEM1, MEM3, MEM4, MEM6, and MEM8). After iteratively excluding environmental variables associated with the highest VIF values until all variables presented a VIF < 20, 10 variables remained: SST_OM (8.20), SST_OSD

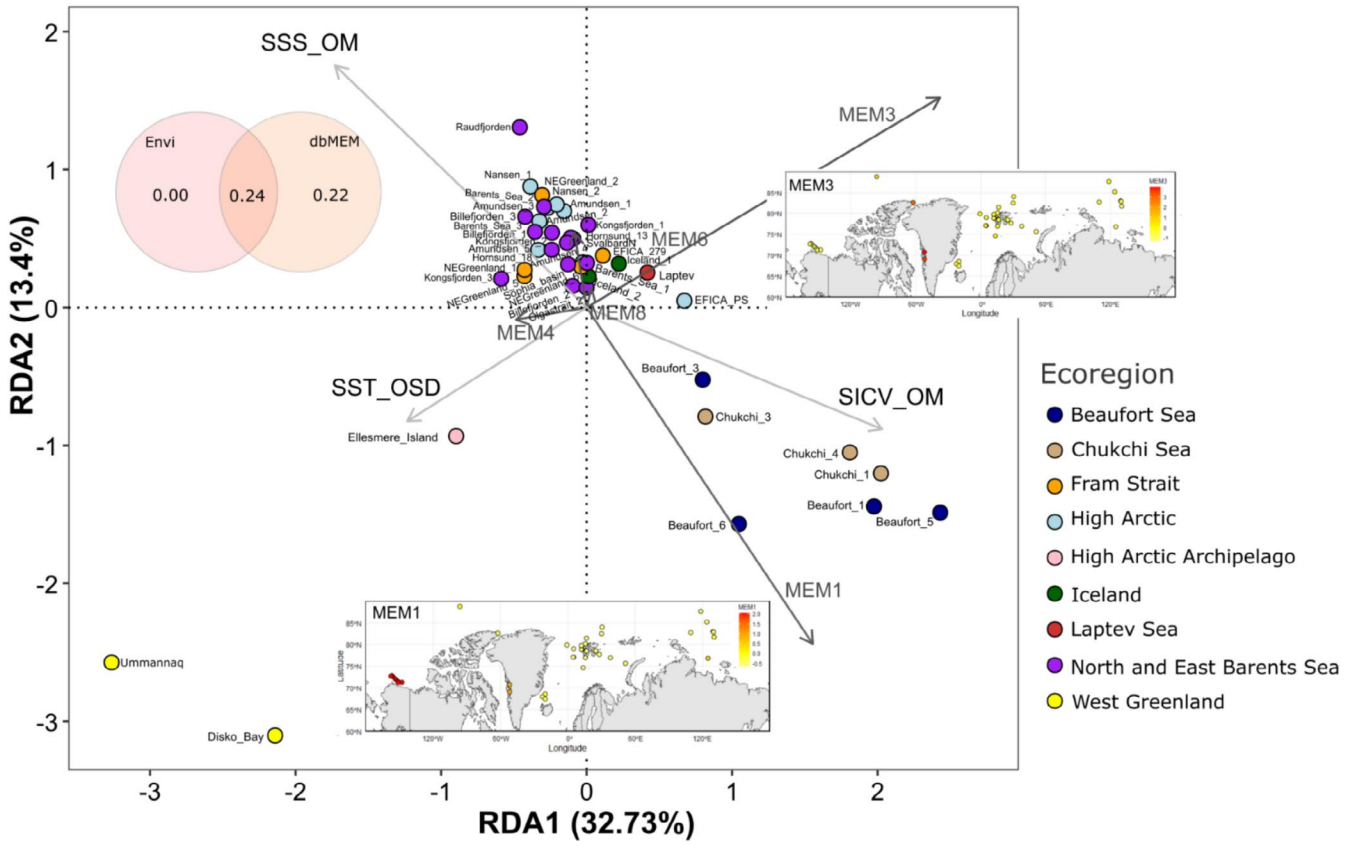

FIGURE 5 | Redundancy analysis plot (RDA) performed with the putatively adaptive SNP loci (35 SNPs) as dependent variables and spatial (db-MEM vectors) and environmental data as explanatory variables. Dots are coloured according to ecoregions. The arrows show the direction in which each explanatory variable is most strongly associated with the RDA axes, and their length is proportional to the associated R^2 adjusted. The Venn Diagram shows the proportion of the variance (as represented by R^2 adjusted) that is attributed solely to the environmental or the spatial (dbMEM) variables, and the proportion that is shared between the two sets of variables (at the intersection). The dbMEM vectors that explain most of the variance, MEM1 and MEM3, are plotted on the map. SICV_OM, overall mean in sea ice current velocity; SSS_OM, overall mean in sea surface salinity; SST_OSD, overall standard deviation in sea surface temperature.

(13.62), SSS_OM (9.39), SSS_OSD (3.85), SIA_WM (12.10), SIA_OSD (13.57), SIT_SM (11.98), SIT_OSD (14.97), SICV_OM (2.67), and MLT_OSD (2.26). Model building using this set of 10 environmental variables in both directions resulted in the selection of three variables: the overall mean in sea ice current velocity (SICV_OM), the overall mean in sea surface salinity (SSS_OM), and the overall standard deviation in sea surface temperature (SST_OSD).

The global RDA using the putatively adaptive dataset and all selected explanatory variables (MEM1, MEM3, MEM6, MEM8, SICV_OM, SSS_OM, and SST_OSD) was significant (p-value = 0.001) and accounted for 46% of the genomic variation (adjusted $R^2 = 0.46$). Of this total explained variation, 22% was attributable to spatial variables only (MEM1, MEM3, MEM6, and MEM8), whereas 24% is a joint effect of spatial structure and the three environmental variables. The first three RDA axes were significant (p-values = 0.001, 0.001 and 0.043). The first RDA axis accounted for 32.7% of the explained variation, whereas the second accounted for 13.4%. Beaufort and Chukchi Sea populations are positively correlated with SICV_OM and MEM1 and negatively correlated with SSS_OM. West Greenland (Disko Bay and Uummannaq) populations are positively correlated with SST_OSD and negatively correlated with MEM3 (Figure 5).

4 | Discussion

Sound knowledge of population connectivity and genetic adaptation can provide insights into the potential resilience of polar cod populations to climate change and other anthropogenic stressors (Geoffroy et al. 2023). Despite the pivotal role of polar cod in Arctic ecosystems, our understanding of how the marine environment shapes its genetic structure remains limited. To close this knowledge gap, we investigated the genomic population structure of polar cod at a circumpolar scale using 922 high-quality SNPs and explored potential drivers of connectivity and adaptation. We uncovered a population genetic structure dominated by large-scale differentiation in three spatial groups: (i) Beaufort–Chukchi seas, (ii) all ecoregions connected by the Transpolar Drift from the Laptev Sea to Iceland, including the European Arctic (hereafter termed TPD + EA group), and (iii) West Greenland. These findings suggest that large-scale oceanographic and sea ice drift features, particularly the Beaufort Gyre and the Transpolar Drift, are major drivers of connectivity. Seascape genetic analyses confirmed that only a small proportion of neutral genetic variation is attributed to spatial structure and environment. The differentiation detected between West Greenland and the other locations is predominantly driven by loci putatively under selection. Variation in putatively adaptive

loci underlined the interaction of spatial patterns and specific regional environmental conditions in driving local adaptation of the Beaufort–Chukchi and West Greenland populations. In addition to the overarching genomic structure, we observed a signature of structural variation independent of ecoregion in three clusters most likely representing two groups of homozygotes and one intermediate group of heterozygotes, suggesting a chromosomal inversion (see Einarsson et al. 2023; Bringloe et al. 2024; Hoff, Maurstad, Le Moan, et al. 2024). In the following sections, we discuss patterns, potential drivers and broader implications of differentiation for each of the three main genetic groups.

4.1 | What Drives the Genomic Structure of Polar Cod in the Arctic Seascape?

4.1.1 | Beaufort and Chukchi Seas

Genetic differentiation of the Beaufort–Chukchi group is observed at putatively adaptive loci, and to a lesser extent neutral loci, suggesting that it is driven by a combination of limited gene flow with adjacent ecoregions and local adaptation. Our Beaufort–Chukchi group corresponds to the 'Alaskan Beaufort and Chukchi seas' cluster of Nelson et al. (2020) that extends south to the Northern Bering Sea (Nelson et al. 2020; Wilson et al. 2020). Similarly, genetically distinct 'Pacific Arctic' populations have been observed for a range of zooplanktonic species like *Thysanoessa inermis* (Euphausiidae; Bucklin et al. 2023), *Eukrohnia hamata* (Chaetognatha; DeHart et al. 2020) and *Limacina helicina* (Pteropoda; Abyzova et al. 2018) and fish species like Greenland halibut *Reinhardtius hippoglossoides* (Orlova et al. 2019) and capelin *Mallotus villosus* (Præbel et al. 2008). Nelson et al. (2020) also uncovered a genetically distinct group of polar cod on the 'Canadian coast of the Beaufort Sea' which corresponds to the 'Western North American Arctic' of Bringloe et al. (2024); samples from this area, however, were not available for our study.

Spawning grounds have been inferred in the northern Bering and southern Chukchi seas (Kono et al. 2016; Vestfals et al. 2021) and along the Alaskan North Slope (Craig et al. 1982). Pacific Water, transporting eggs and larvae to the Chukchi Plateau, may follow two pathways. The main branch enters the deep Central Arctic basins and recirculates in the Amerasian Basin with the Beaufort Gyre (Figure 6B). At its northwestern limit, the Beaufort Gyre merges with the Transpolar Drift. A limited amount of Pacific Water follows the second pathway, flowing eastward along the Alaskan coast to feed into the Canadian Arctic Archipelago (Hu et al. 2019; Jones et al. 1998; Figure 6B). These large-scale water and sea ice circulation patterns would explain: (i) genetic distinctiveness of the 'Bering-Beaufort-Chukchi' population, with putative spawning grounds in the northern Bering and southern Chukchi seas and potential dispersal offshore via the Beaufort Gyre, where sea ice may remain trapped for years (Figures 3A,B and 6), (ii) admixture between the 'Bering-Beaufort-Chukchi' and the 'TPD + EA' clusters, especially off the Laptev Sea, where the Beaufort Gyre joins the Transpolar Drift (Figures 3A,B and 6) and (iii) genetically distinct populations on the Alaskan and western Canadian coasts (Nelson et al. 2020), due to limited oceanographic connectivity. The latter might also explain the spatial separation of eastern and western aggregations of small polar cod in the Beaufort Sea, indicating that polar cod in the eastern Beaufort Sea likely did not originate in the Chukchi Sea (Forster et al. 2020).

Genetic variation of the Beaufort–Chukchi population is positively associated with geographic distance and ice-related variables, including mean winter sea ice area fraction, variability in sea ice thickness and mean sea ice current velocity and negatively correlated to mean sea surface salinity (Figure 5 and Appendix S11). The Chukchi and Beaufort seas are heavily covered with ice in winter. Sea ice velocity is particularly high (see maps in Appendix S12), as the Alaskan coastal current combines with the Central Channel to form a strong and narrow jet flowing eastward along the Beaufort Shelf (Pickart 2004; Winsor and Chapman 2004). The Beaufort and Chukchi seas are also characterised by lower salinity surface water than other ecoregions due to freshwater discharge from the Mackenzie River and low-salinity Pacific inflow from the Bering Strait (Crawford et al. 2012). However, salinity is likely not a limiting factor, as polar cod in this region are found in a wide range of salinities (15–34 ppt; Crawford et al. 2012). Environmental extremes and high variability in regional ice cover, temperature, light, freshwater, turbidity, and currents may foster specific adaptations of the local biota (Carmack and Macdonald 2002). A longer open-water season, thinning ice cover and strengthening of the Beaufort Gyre result in habitat and food web alterations, putatively inducing selective pressures on the local polar cod populations (Peng and Meier 2018; Steiner et al. 2021; Thomson et al. 2016).

4.1.2 | Transpolar Drift and European Arctic

Our TPD + EA group corresponds to Nelson et al. (2020)'s group spanning the Siberian shelves, Fram Strait and Iceland. Similar patterns of genetic homogeneity across the TPD have been observed in the zooplankton species *E. hamata* (DeHart et al. 2020) and *L. helicina* (Abyzova et al. 2018), and Greenland halibut (Orlova et al. 2019).

Sea ice from the western Siberian Seas is entrained in the Transpolar Drift current and exported into the Barents Sea and eastern Fram Strait (Pfirman et al. 2004); some sea ice may also reach waters off Ellesmere Island (Kwok et al. 2013). Polar cod have been recorded in large numbers in the Amundsen and Nansen basins under ice that originated from the Laptev and Kara seas (David et al. 2016). The genetically homogeneous 'TPD + EA' cluster supports the 'Transpolar Drift hypothesis' by David et al. (2016), which implies that young polar cod are advected with the Transpolar sea ice Drift from the Siberian shelf across the Arctic Ocean up to spawning grounds in the Svalbard archipelago, Barents and Greenland seas and further to Iceland (Figures 3A,B, 4A and 6; David et al. 2016; Melnikov and Chernova 2013; Pettitt-Wade et al. 2021).

Despite high connectivity, the geographically large TPD + EA group shows evidence of weak but significant population substructuring. In particular, polar cod sampled in the Laptev Sea is weakly differentiated from adjacent ecoregions (Figures 2 and 4B). Similarly, previous studies observed differentiation between the East Siberian and Laptev seas and the Kara Sea

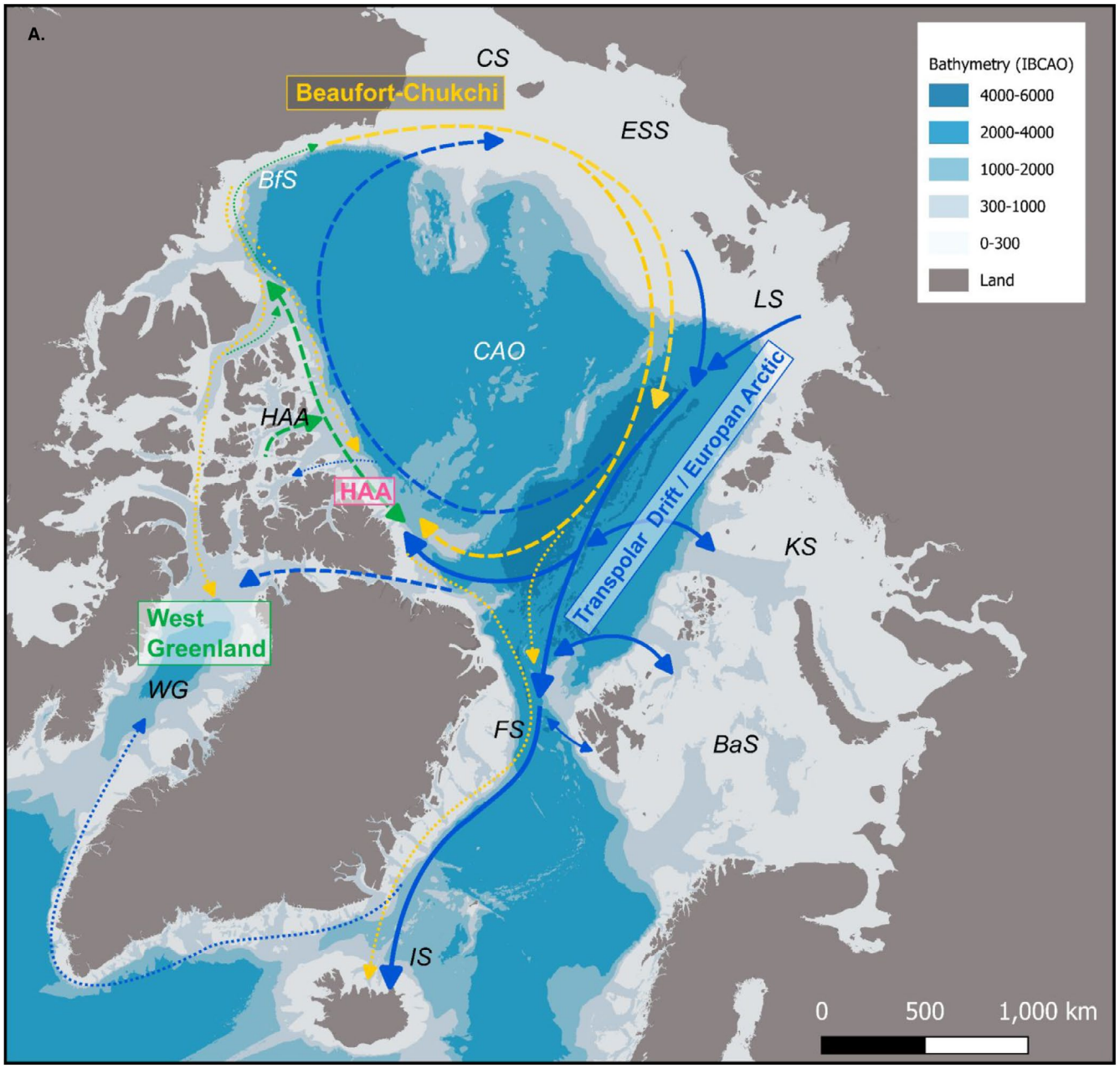

FIGURE 6 | (A) Connectivity between genetic groups of polar cod in the Arctic Ocean, as identified by the statistical approaches used in this study for the full 922 SNPs dataset (Figures 3A and 4). Three genetically differentiated groups are indicated: Transpolar Drift/European Arctic (TPD + EA; blue), West Greenland (green) and Beaufort and Chukchi seas (yellow). Arrows indicate potential gene flow between regions sampled in this study, as indicated by our analyses (Figure 3) and considering major currents and sea ice drift shown in (B). The arrows are colour-coded according to the genetic grouping at their origin. Full arrows indicate close connectivity within the TPD + EA grouping. Dashed arrows indicate weak gene flow between the different groupings. Dotted arrows indicate very weak gene flow between groupings. The biogeographical regions of the Arctic Ocean, as shown in Figure 1, are BaS, Barents Sea; BfS, Beaufort Sea; CS, Chukchi Sea; ESS, east Siberian Sea; FS, Fram Strait; HAA, High Arctic Archipelago; IS, Iceland; KS, Kara Sea; LS, Laptev Sea; WG, West Greenland. (B) Major ocean currents and sea ice drift in the Arctic Ocean, redrawn after Bluhm et al. (2015) and Geoffroy et al. (2023). Warm currents are shown in red, cold currents in white. The Arctic Boundary Current (ABC) transports warm Atlantic Water along the slopes around the Arctic Ocean at intermediate depths (approximately 100–1000 m). The transpolar drift (TPD) and the Beaufort Gyre (BG) are the two major wind-driven surface current systems advecting sea ice with underlying cold water over the Central Arctic Ocean (CAO). From the Bering Strait, warm Bering Sea water (BS) is advected into the CAO. Cold surface currents connect the Beaufort shelf and the CAO with the High Arctic Archipelago and West Greenland. Bathymetry: International Bathymetric Chart of the Arctic Ocean (IBCAO, www.gebco.net).

(Gordeeva and Mishin 2019; 7 microsatellites) and Svalbard (Quintela et al. 2021; 116 SNPs) as a result of isolation-by-distance. Furthermore, the Icelandic population showed low but significant differentiation from neighbouring ecoregions (Figures 2 and 4B). A similar genetic discontinuity has been observed in Greenland halibut (Vihtakari et al. 2022; Westgaard

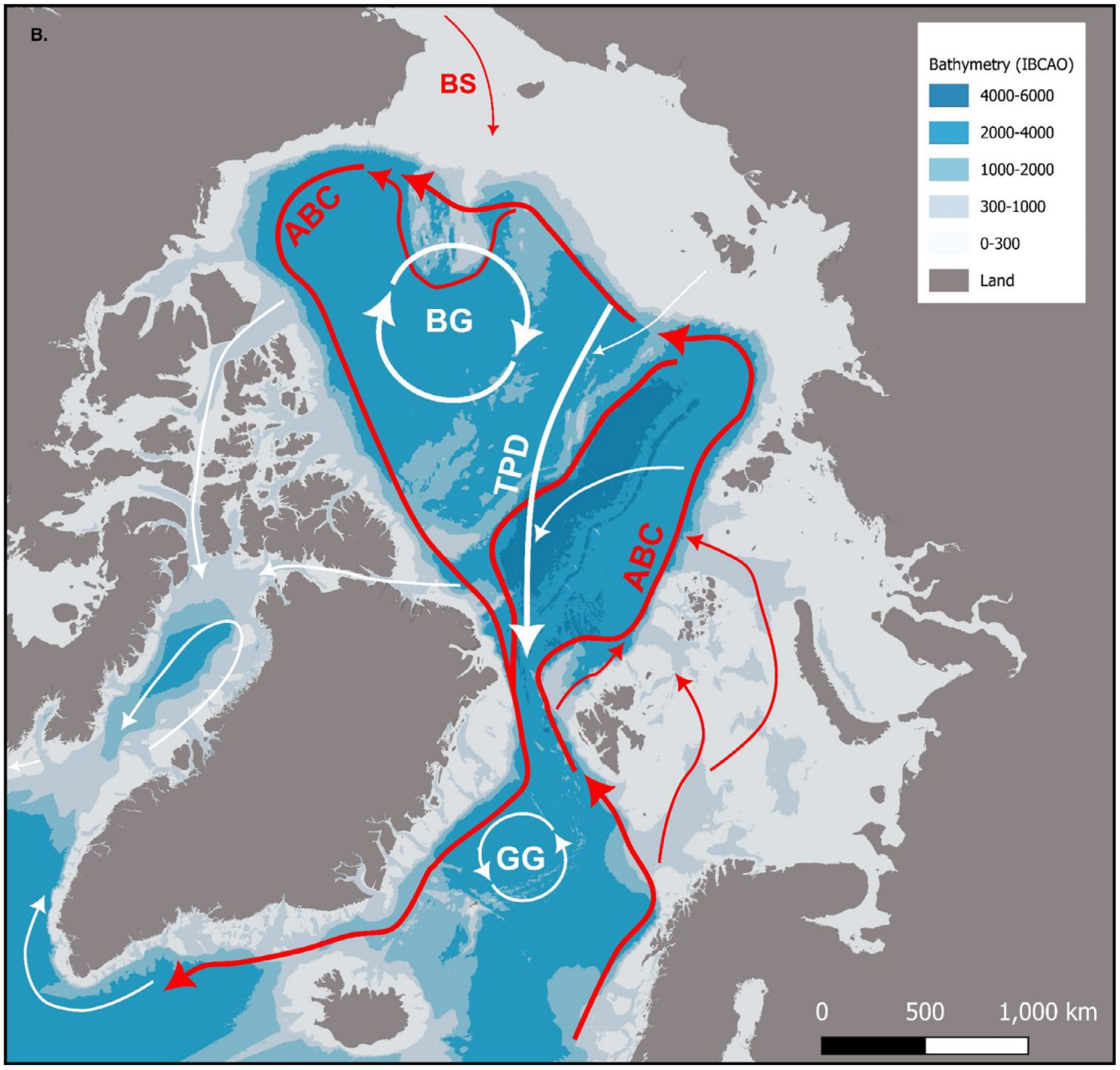

FIGURE 6 | (Continued)

et al. 2017), beaked redfish *Sebastes mentella* (Saha et al. 2017), Atlantic haddock *Melanogrammus aeglefinus* (Berg et al. 2021) and Atlantic cod *Gadus morhua* (Johansen et al. 2020).

In the Svalbard and Barents Sea region, field observations suggest at least two spawning grounds, one in the vicinity of Svalbard (on the eastern side and in the western fjords) and another one in the Pechora Sea southwest of Novaya Zemlya (Aune et al. 2021; Korshunova 2012). Most populations in the Svalbard fjords are not significantly differentiated from each other, Fram Strait, and the High Arctic, which confirms previous results using microsatellite markers (Maes et al. 2021). Dispersal models show that eggs released in the western fjords of Svalbard are mostly retained, and that offshore transport occurs from the putative Svalbard spawning areas into Fram Strait and to the northeast along the shelf edge of the polar basin (Eriksen et al. 2020; Gjøsæter et al. 2020). Polar cod on the eastern side of the archipelago ('Svalbard East' and 'Barents Sea') indeed show higher levels of differentiation (F_{ST} values up to 0.013) from the western Svalbard fjords (Figures 1 and 2). These polar cod might originate from spawning grounds in the Pechora Sea, from where eggs drift northward along Novaya Zemlya and westward in the Barents Sea (Huserbråten et al. 2019).

We did not find evidence for local adaptation in the TPD + EA group. However, the contrasting environmental conditions in Western Svalbard fjords and northeastern Barents Sea (i.e., influenced by different water masses; Eriksen et al. 2020) may lead to locally adapted populations. The exploration of potential adaptive divergence in these regions requires high-density sampling, phenotyping, and environmental modelling (Dauphin et al. 2023; Riginos et al. 2016).

4.1.3 | West Greenland

The population off West Greenland represents a distinct genetic cluster based on putatively adaptive loci (Figure 3C), which cannot be separated from the TPD + EA cluster with only neutral loci (Figure 3B). Therefore, genetic differentiation of the West Greenland ecoregion is largely driven by local adaptation concurrent with high gene flow. Local adaptation may occur in the presence of genetic connectivity between populations if the strength of selection overcomes the homogenising effect of gene flow (Hellberg 2009). Genetic connectivity between West Greenland and the Northeast Atlantic Ocean has been inferred for other species, including *T. inermis* (Bucklin et al. 2023), *E. hamata* (DeHart et al. 2020), *M. villosus* (Præbel et al. 2008) and *R. hippoglossoides* (Roy et al. 2014; Vis et al. 1997). It remains to be investigated whether polar cod from 'the eastern coastline of Canada' group of Nelson et al. (2020) and the 'East North American Arctic' cluster of Bringloe et al. (2024) belong to the same genetic group as our 'West Greenland' samples, collected on the opposite side of Baffin Bay.

Genetic exchange with the TPD + EA population may occur by advection of fish from the TPD through the High-Arctic Archipelago. Connectivity between the Labrador Sea and the East Greenland coast might also occur via the East and West Greenland currents (Figure 6). Larvae and ready-to-spawn polar cod observed in East Greenland fjords suggest the presence of several spawning grounds along the coast (Astthorsson 2016). Furthermore, sea ice originating from the Arctic Ocean annually drifts along this coast (Blindheim and Osterhus 2005) and may facilitate some genetic exchange around the southern tip of Greenland. Dispersal from the Pacific Arctic to West Greenland may also occur via the Northwest Passage, as polar cod larvae were found in high densities in the eastern Parry Channel and Peel Sound (Bouchard et al. 2018). Such connectivity patterns might explain the higher ancestry of some individuals in West Greenland to the genetic cluster in the Beaufort–Chukchi seas compared to TPD + EA ecoregions.

The genetic differentiation of the West Greenland group is positively correlated with the spatial structure and the variability in sea surface temperature (Figure 5). West Greenland fjords are located at the southern border of sea ice and are influenced by both sub-Arctic waters from southwestern Greenland and Arctic waters within the Labrador Sea (Gladish et al. 2015; Rysgaard et al. 2020). The area has a pronounced seasonality and large interannual variation in terms of sea surface temperature and sea ice cover (see maps in Appendix S12; Carroll et al. 2018; Møller et al. 2023). Warm years have been associated with partial recruitment failures in polar cod (Bouchard et al. 2021). Although the area might be important for spawning and larval retention (Melnikov and Chernova 2013; Bouchard et al. 2023), it is, nowadays, likely a suboptimal nursery ground, at the upper limit of their thermal tolerance (Bouchard et al. 2021; Geoffroy et al. 2023).

4.1.4 | Chromosomal Rearrangements

In addition to the overarching genomic structure, we observed a putative signature of chromosomal rearrangement. The three clusters of individuals observed in the PCA using PCAdapt outlier SNPs (Appendix S10) most likely represent two groups of homozygotes and one intermediate group of heterozygotes (Huang et al. 2019; Mérot 2020). The clusters are not geographically structured; hence, other drivers influence the distribution of these genotypes. A similar pattern was observed in polar cod from the Barents and Kara seas by Quintela et al. (2021) and from the Western Arctic to the Gulf of St. Lawrence ecoregions by Bringloe et al. (2024). Additional research attributed such a pattern in polar cod to chromosomal inversions, linked to sex and putatively to ecotype (Bringloe et al. 2024). In a most recent development, the reference genome of polar cod revealed several chromosomal inversions and fusions (Hoff, Maurstad, Tørresen, et al. 2024). Whole-genome population sequencing of polar cod samples collected in the Barents Sea, supported by the reference genome, has identified five subclusters without a clear geographical pattern (Hoff, Maurstad, Le Moan, et al. 2024). Inversions are commonly linked to phenotypes, such as migratory behaviour (Sodeland et al. 2016) and morphotype (Jones et al. 2012). Hence, inversions might foster adaptive divergence under high gene flow (Kirubakaran et al. 2016) and might have facilitated the evolution of distinct local and regional genotypes in polar cod (Madsen et al. 2016; Hoff, Maurstad, Le Moan, et al. 2024), albeit so far with unknown adaptive implications.

4.2 | Prospects of Polar Cod in a Shifting Seascape

Polar cod are facing a range of environmental pressures related to climate change and increasing anthropogenic activities. Among these stressors, sea ice decline stands out as a critical threat, influencing the survival and dispersal of early life stages (Geoffroy et al. 2023). The present study shows that the genetic structure of polar cod can be explained by the main surface currents and sea ice drift patterns, driven by the Beaufort Gyre and the Transpolar Drift (Figure 6). Young sympagic polar cod are likely an important vector of genetic connectivity across the Central Arctic basin (David et al. 2016; Melnikov and Chernova 2013). During their year-long drift, the under-ice habitat provides a unique combination of low energetic cost due to subzero temperatures and lipid-rich prey, which would not be available in open waters, particularly during the polar night (Flores et al. 2023; Kohlbach et al. 2017; Schaafsma et al. 2024). The ongoing sea ice decline is therefore likely to have profound impacts on the circumpolar connectivity and size of polar cod populations.

Lower genetic diversity through reduced connectivity with other populations and collapsing population sizes may further decrease resilience to environmental change. The TPD + EA population, which does not reproduce in the CAO, may suffer from reduced advection from the Siberian shelf because sea ice formation is increasingly propagating further offshore, away from spawning grounds (Krumpen et al. 2019). Although adult dispersal might be less affected, the loss of spawning and nursery habitat will have consequences for the entire population. This will reduce gene flow from the Transpolar Drift system to the High Arctic Archipelago and the Beaufort Gyre, but also the European Arctic, including Iceland and Greenland (Figure 6). Survival is expected to be lower in the Atlantic Arctic region, which has been estimated to face the greatest pressure from climate change compared to other domains of the Arctic Ocean (Geoffroy

et al. 2023). Southern populations like the Icelandic and West Greenland ones are not only threatened by ocean warming, potentially resulting in either extinction or displacement towards colder, more northern latitudes (Astthorsson 2016), but might become more endemic due to the constrained gene flow from other regions, resulting in decreased genetic diversity. Polar cod populations in the CAO and the High Arctic Archipelago might face the lowest risk from climate change (Geoffroy et al. 2023). However, the strong dependency of the CAO population on advection of juveniles from the Eurasian shelf and the potential negative impact of reduced connectivity on the resilience of the population in the High Arctic Archipelago indicates that even these potential refugia populations may become more impacted by climate change than previously assumed. While the disappearing multiyear ice (Wood et al. 2015) and expanding Beaufort Gyre (Regan et al. 2019) in the Canadian Arctic might transiently favour genetic exchanges between the eastern and western populations (Bouchard et al. 2018), in the longer term, the complete disappearance of summer ice is likely to result in reduced genetic connectivity and reduced population sizes.

With genetic sub-structuring, the risk of overfishing of local stocks increases (Bonanomi et al. 2015; Knutsen et al. 2018). Historically, polar cod has experienced periods of high fishing pressure in the Exclusive Economic Zone to the extent that fishing moratoria were declared (Geoffroy et al. 2023). Multiple examples of the negative impact of chronic overfishing on genetic diversity and stock collapse have been documented (Pinsky and Palumbi 2014). Current fisheries are limited to coastal fishing by indigenous communities and bycatch from commercial trawling. Increasing accessibility of the Arctic Ocean, however, may change this situation (Niiranen et al. 2018). In the longer term, polar cod may benefit from the fishing moratorium in the CAO implemented by the Agreement to prevent Unregulated High Seas Fisheries in the Central Arctic Ocean for the next 13 years (Calderwood and Ulmer 2023). This precautionary measure ensures that sufficient information on fish stocks and ecosystem dynamics will be collected to establish environmentally and economically sustainable resource management (Pan and Huntington 2016).

The Arctic Council has adopted a framework for a pan-Arctic network of Marine Protected Areas (MPA) for which polar cod serves as a key target species due to its central role in the Arctic food web (Geoffroy et al. 2023; PAME 2015; PAME et al. 2017). Our analysis shows that the spatial design of such an MPA network should account for the protection of all genetic groups to help preserve genetic diversity and connectivity for the whole population. In this regard, regions of high genetic exchange such as the High Arctic Archipelago as well as potential spawning areas of major genetic groups such as the Bering–Chukchi–Beaufort seas, Baffin Bay, the Pechora Sea, and the Laptev Sea may prove highly valuable for the protection of polar cod in a changing Arctic Ocean. The MPAs may contribute to frameworks for decision-making under a regime of global uncertainty.

Author Contributions

Sarah M. Maes, Henrik Christiansen and Hauke Flores conceptualised the study. Sarah M. Maes, Caroline Bouchard, Felix C. Mark, Torild Johansen, Daria Zelenina, Magnus Lucassen, Anna H. Ólafsdóttir, and Hauke Flores collected the samples. Sarah M. Maes and Bart Hellemans created the data. Sarah M. Maes, Marie L. Verheye and Henrik Christiansen analysed the data and interpreted the findings with bioinformatic support from Enora Geslain. Marie L. Verheye wrote the first draft of the manuscript with contributions from Sarah M. Maes. Sarah M. Maes, Marie L. Verheye, Filip A. M. Volckaert, Henrik Christiansen and Hauke Flores contributed to the interpretation of the findings; all authors revised the final draft.

Acknowledgements

This work was made possible by indispensable field support from Fokje Schaafsma, Michiel van Dorssen, Benjamin Lange, Martina Vortkamp, Antonia Immerz, Erik Sulanke, Kim Vane, Elisa Bravo-Rebolledo, Nils Koschnick, Jennifer Steffen, Erin Kunisch, Mai Apasiri Klasmeier, Nadya Zakharova, Ron ten Boer, Franz Mueter, Jared Weems, Alexei Pinchuk, Lorena Edenfield, Kristina Kunz, Nicole Hildebrandt, Anders Svensson, Giulia Castellani, Serdar Sakinan and Katrin Schmidt. Sarah M. Maes benefited from a fellowship for strategic basic research from the Research Foundation—Flanders (Belgium; grant no. 1S04418N). Marie L. Verheye benefited from postdoctoral funding from EU tender EFICA (contract no. EASME/EMFF/2018/003). Henrik Christiansen was supported by a fellowship from the former Flemish Agency for Innovation by Science and Technology, now Flanders Innovation and Entrepreneurship (VLAIO, grant 141328). Research of Sarah M. Maes, Marie L. Verheye, Enora Geslain and Henrik Christiansen was supported by research infrastructure grant I001621N of EMBRC Belgium—Research Foundation Flanders. The GO-WEST team and expedition were supported by ARICE grant 730965, Bureau of Ocean Energy Management (BOEM) Award #M19AC00018 and the University of Alaska Fairbanks (ship time). Research was funded by the Helmholtz Association Research Programme Polar regions and Coasts in the changing Earth System II (PACES II), Topic 1, WP 4 and is part of the Helmholtz Association Young Investigators Group *Iceflux*: Ice-ecosystem carbon flux in polar oceans (VH-NG-800) and the EU EFICA project. The SUIT net was developed by Wageningen Marine Research (formerly IMARES) with support from the Netherlands Ministry of Agriculture, Nature and Food Quality (projects WOT-04-009-036 and WOT-04-009-047.04) and the Netherlands Polar Programme (NWO project 866.13.009), which also supported research during RV *Polarstern* expeditions PS80 and PS92. PS122 data used in this manuscript were produced as part of the international Multidisciplinary drifting Observatory for the Study of the Arctic Climate (MOSAiC) with the tag MOSAiC20192020. Work during MOSAiC, PS92 and PS106 was funded by the Dutch Research Council grants 866.18.003 and 866.13.009. The authors thank chief scientists Antje Boetius and Ilka Peeken, captains Uwe Pahl and Thomas Wunderlich and the crew of *Polarstern* expedition PS80 *IceArc*, PS92 *TRANSSIZ*, PS106 *SiPCA* and PS122 *MOSAiC* for their support (expedition grants: AWI-PS80_01, AWI_PS92_01, AWI_PS106/1_2_00 and AWI_PS122_00). We also thank captain Eric Piper, chief scientist Jim Thomson (University of Washington) and the crew of RV *Sikuliaq* for their support and expertise. The Genomics Core Leuven (Belgium) performed the high-throughput DNA sequencing. We thank Hugo Gante for helpful insights on genetic structurer and Sissel Jentoft and Siv Hoff for helpful insights on chromosomal inversions. This publication has benefited from insights initiated as part of COST Action CA19107 SEA-UNICORN, supported by COST (European Cooperation in Science and Technology, https://www.cost.eu).

Disclosure

Benefit-sharing statement: Benefits from this research accrue from the sharing of our data and results on public databases as described above.

Ethics Statement

Polar cod from Svalbard, the Sophia Basin and the CAO were sampled and processed according to and within the laws, guidelines and policies of the German Animal Welfare Organisation. No specific permissions

were required. Sampling in US waters was approved by the Institutional Animal Care and Use Committee of the University of Alaska Fairbanks. Polar cod collection in Greenland were permitted through non-exclusive licences no. G19-013, G19-036, and G24-003 for utilization of Greenland Genetic Resources (Prior informed consent under the Biological Diversity Convention and the Nagoya Protocol) issued by the Government of Greenland, Ministry of Business, Trade, Mineral Resources, Justice and Gender Equality. Polar cod were sacrificed immediately after sampling.

Conflicts of Interest

The authors declare no conflicts of interest.

Data Availability Statement

The raw reads data sets are available on the NCBI Sequence Read Archive (SRA) under Bioproject PRJNA1205545, accession numbers SRX27229408 to SRX27229411. SNP, environmental, and allele frequencies data sets used in the RDA are openly available in Dryad at https://doi.org/10.5061/dryad.fqz612k30. Occurrence metadata are cross-linked on the Global Biodiversity Information Facility (www.GBIF.com).

References

Abyzova, G. A., M. A. Nikitin, O. V. Popova, and A. F. Pasternak. 2018. "Genetic Population Structure of the Pelagic Mollusk *Limacina helicina* in the Kara Sea." *PeerJ* 6: e5709.

Andrello, M., D. Mouillot, S. Somot, W. Thuiller, and S. Manel. 2015. "Additive Effects of Climate Change on Connectivity Between Marine Protected Areas and Larval Supply to Fished Areas." *Diversity and Distributions* 21, no. 2: 139–150.

Andrews, S. 2010. *FastQC: A Quality Control Tool for High Throughput Sequence Data*. Babraham Bioinformatics, Babraham Institute.

Astthorsson, O. S. 2016. "Distribution, Abundance and Biology of Polar Cod, *Boreogadus saida*, in Iceland–East Greenland Waters." *Polar Biology* 39, no. 6: 995–1003.

Aune, M., E. Raskhozheva, H. Andrade, et al. 2021. "Distribution and Ecology of Polar Cod (*Boreogadus saida*) in the Eastern Barents Sea: A Review of Historical Literature." *Marine Environmental Research* 166: 105262.

Beaumont, M. A., and D. J. Balding. 2004. "Identifying Adaptive Genetic Divergence Among Populations From Genome Scans." *Molecular Ecology* 13, no. 4: 969–980.

Berg, P. R., P. E. Jorde, K. A. Glover, et al. 2021. "Genetic Structuring in Atlantic Haddock Contrasts With Current Management Regimes." *ICES Journal of Marine Science* 78, no. 1: 1–13.

Berge, J., Ø. Varpe, M. A. Moline, et al. 2012. "Retention of Ice-Associated Amphipods: Possible Consequences for an Ice-Free Arctic Ocean." *Biology Letters* 8, no. 6: 1012–1015.

Blindheim, J., and S. Osterhus. 2005. "The Nordic Seas, Main Oceanographic Features." *Geophysical Monograph-American Geophysical Union* 158: 11.

Bluhm, B. A., K. N. Kosobokova, and E. C. Carmack. 2015. "A Tale of Two Basins: An Integrated Physical and Biological Perspective of the Deep Arctic Ocean." *Progress in Oceanography* 139: 89–121.

Bogan, S. N., J. Johns, J. S. Griffiths, et al. 2023. "A Dynamic Web Resource for Robust and Reproducible Genomics in Nonmodel Species: marineomics.io." *Methods in Ecology and Evolution* 14: 2709–2716. https://doi.org/10.1111/2041-210X.14219.

Bonanomi, S., L. Pellissier, N. O. Therkildsen, et al. 2015. "Archived DNA Reveals Fisheries and Climate Induced Collapse of a Major Fishery." *Scientific Reports* 5, no. 1: 15395.

Borcard, D., and P. Legendre. 2002. "All-Scale Spatial Analysis of Ecological Data by Means of Principal Coordinates of Neighbour Matrices." *Ecological Modelling* 153, no. 1–2: 51–68.

Bouchard, C., A. Charbogne, F. Baumgartner, and S. M. Maes. 2021. "West Greenland Ichthyoplankton and How Melting Glaciers Could Allow Arctic Cod Larvae to Survive Extreme Summer Temperatures." *Arctic Science* 7, no. 1: 217–239. https://doi.org/10.1139/as-2020-0019.

Bouchard, C., P. Farnole, K. Lynge-Pedersen, P. E. Dahl, and H. Christiansen. 2023. "Arctic Cod (*Boreogadus saida*) in Fjord and Glacial Habitats: A Collaborative Study With Uummannap Kangerlua Fishers." *Arctic Science* 9, no. 4: 781–795.

Bouchard, C., M. Geoffroy, M. LeBlanc, and L. Fortier. 2018. "Larval and Adult Fish Assemblages Along the Northwest Passage: The Shallow Kitikmeot and the Ice-Covered Parry Channel as Potential Barriers to Dispersal." *Arctic Science* 4, no. 4: 781–793.

Bradstreet, M. S., and W. E. Cross. 1982. "Trophic Relationships at High Arctic Ice Edges." *Arctic* 35: 1–12.

Bringloe, T. T., A. Bourret, D. Cote, et al. 2024. "Genomic Architecture and Population Structure of *Boreogadus saida* From Canadian Waters." *Scientific Reports* 14: 19331. https://doi.org/10.1038/s41598-024-69782-w.

Brodersen, J., and O. Seehausen. 2014. "Why Evolutionary Biologists Should Get Seriously Involved in Ecological Monitoring and Applied Biodiversity Assessment Programs." *Evolutionary Applications* 7, no. 9: 968–983.

Bucklin, A., J. M. Questel, P. G. Batta-Lona, et al. 2023. "Population Genetic Diversity and Structure of the Euphausiids *Thysanoessa inermis* and *T. raschii* in the Arctic Ocean: Inferences From COI Barcodes." *Marine Biodiversity* 53, no. 5: 70.

Calderwood, C., and F. A. Ulmer. 2023. "The Central Arctic Ocean Fisheries Moratorium: A Rare Example of the Precautionary Principle in Fisheries Management." *Polar Record* 59: e1.

Carmack, E. C., and R. W. Macdonald. 2002. "Oceanography of the Canadian Shelf of the Beaufort Sea: A Setting for Marine Life." *Arctic* 55, no. Suppl 1: 29–45.

Carroll, D., D. A. Sutherland, B. Curry, et al. 2018. "Subannual and Seasonal Variability of Atlantic-Origin Waters in Two Adjacent West Greenland Fjords." *Journal of Geophysical Research: Oceans* 123, no. 9: 6670–6687.

Catchen, J., P. A. Hohenlohe, S. Bassham, A. Amores, and W. A. Cresko. 2013. "Stacks: An Analysis Tool Set for Population Genomics." *Molecular Ecology* 22, no. 11: 3124–3140.

Chan, K. Y. K., M. A. Sewell, and M. Byrne. 2018. "Revisiting the Larval Dispersal Black Box in the Anthropocene." *ICES Journal of Marine Science* 75, no. 6: 1841–1848. https://doi.org/10.1093/icesjms/fsy097.

Chernova, N. V., V. A. Spiridonov, V. L. Syomin, and M. V. Gavrilo. 2021. "Notes on the Fishes of the Severnaya Zemlya Archipelago and the Spawning Area of Polar Cod *Boreogadus saida* (Gadidae)." *Труды Зоологического Института РАН* 325, no. 2: 248–268.

Cottier, F. R., F. Nilsen, R. Skogseth, V. Tverberg, J. Skarðhamar, and H. Svendsen. 2010. "Arctic Fjords: A Review of the Oceanographic Environment and Dominant Physical Processes." *Geological Society, London, Special Publications* 344, no. 1: 35–50.

Craig, P. C., W. B. Griffiths, L. Haldorson, and H. McElderry. 1982. "Ecological Studies of Arctic Cod (*Boreogadus saida*) in Beaufort Sea Coastal Waters, Alaska." *Canadian Journal of Fisheries and Aquatic Sciences* 39, no. 3: 395–406.

Crawford, A., J. Stroeve, A. Smith, and A. Jahn. 2021. "Arctic Open-Water Periods Are Projected to Lengthen Dramatically by 2100." *Communications Earth & Environment* 2, no. 1: 109.

Crawford, D. L., and M. F. Oleksiak. 2016. "Ecological Population Genomics in the Marine Environment." *Briefings in Functional Genomics* 15, no. 5: 342–351.

Crawford, R. E., S. Vagle, and E. C. Carmack. 2012. "Water Mass and Bathymetric Characteristics of Polar Cod Habitat along the Continental Shelf and Slope of the Beaufort and Chukchi Seas." *Polar Biology* 35: 179–190. https://doi.org/10.1007/s00300-011-1051-9.

Crooks, K. R., and M. Sanjayan. 2006. *Connectivity Conservation*. Vol. 14. Cambridge University Press.

Dabney, A., J. D. Storey, and G. R. Warnes. 2010. "Qvalue: Q-Value Estimation for False Discovery Rate Control." *R Package Version*, 1(0).

Danecek, P., A. Auton, G. Abecasis, et al. 2011. "The Variant Call Format and VCFtools." *Bioinformatics* 27, no. 15: 2156–2158.

Dauphin, B., C. Rellstab, R. O. Wüest, et al. 2023. "Re-Thinking the Environment in Landscape Genomics." *Trends in Ecology & Evolution* 38, no. 3: 3261–3274.

David, C., B. Lange, T. Krumpen, F. Schaafsma, J. A. van Franeker, and H. Flores. 2016. "Under-Ice Distribution of Polar Cod *Boreogadus saida* in the Central Arctic Ocean and Their Association With Sea-Ice Habitat Properties." *Polar Biology* 39: 981–994.

DeHart, H. M., L. Blanco-Bercial, M. Passacantando, J. M. Questel, and A. Bucklin. 2020. "Pathways of Pelagic Connectivity: *Eukrohnia hamata* (Chaetognatha) in the Arctic Ocean." *Frontiers in Marine Science* 7: 396.

Doherty, P. J., S. Planes, and P. Mather. 1995. "Gene Flow and Larval Duration in Seven Species of Fish From the Great Barrier Reef." *Ecology* 76, no. 8: 2373–2391. https://doi.org/10.2307/2265814.

Einarsson, A. W., E. Árnason, and K. Halldórsdóttir. 2023. "Genomic Evidence for Large Inversions in the Polar Cod *Boreogadus saida* at Similar Chromosomal Locations as Found in Atlantic Cod *Gadus morhua*." Preprint. https://doi.org/10.21203/rs.3.rs-3097434/v1.

Elshire, R. J., J. C. Glaubitz, Q. Sun, et al. 2011. "A Robust, Simple Genotyping-By-Sequencing (GBS) Approach for High Diversity Species." *PLoS One* 6: e19379. https://doi.org/10.1371/journal.pone.0019379.

Eriksen, E., M. Huserbråten, H. Gjøsæter, F. Vikebø, and J. Albretsen. 2020. "Polar Cod Egg and Larval Drift Patterns in the Svalbard Archipelago." *Polar Biology* 43: 1029–1042.

Evanno, G., S. Regnaut, and J. Goudet. 2005. "Detecting the Number of Clusters of Individuals Using the Software STRUCTURE: A Simulation Study." *Molecular Ecology* 14: 2611–2620.

Fevolden, S. E., and J. S. Christiansen. 1997. "Allozymic and scnDNA Homogeneity in Polar Cod (*Boreogadus saida*) (Gadiformes: Gadidae)." *Cybium* 21, no. 4: 411–414.

Flores, H., G. Veyssière, G. Castellani, et al. 2023. "Sea-Ice Decline Could Keep Zooplankton Deeper for Longer." *Nature Climate Change* 13, no. 10: 1122–1130.

Foll, M., and O. Gaggiotti. 2008. "A Genome-Scan Method to Identify Selected Loci Appropriate for Both Dominant and Codominant Markers: A Bayesian Perspective." *Genetics* 180, no. 2: 977–993.

Forster, C. E., B. L. Norcross, F. J. Mueter, E. A. Logerwell, and A. C. Seitz. 2020. "Spatial Patterns, Environmental Correlates, and Potential Seasonal Migration Triangle of Polar Cod (*Boreogadus saida*) Distribution in the Chukchi and Beaufort Seas." *Polar Biology* 43: 1073–1094.

Gagnaire, P.-A. 2020. "Comparative Genomics Approach to Evolutionary Process Connectivity." *Evolutionary Applications* 13, no. 6: 1320–1334.

Gascard, J.-C., J. Zhang, and M. Rafizadeh. 2019. "Rapid Decline of Arctic Sea Ice Volume: Causes and Consequences." *Cryosphere Discussions*: 1–29. https://doi.org/10.5194/tc-2019-2.

Geoffroy, M., C. Bouchard, H. Flores, et al. 2023. "The Circumpolar Impacts of Climate Change and Anthropogenic Stressors on Arctic Cod (*Boreogadus saida*) and Its Ecosystem." *Elementa: Science of the Anthropocene* 11, no. 1: 97.

Geoffroy, M., D. Robert, G. Darnis, and L. Fortier. 2011. "The Aggregation of Polar Cod (*Boreogadus saida*) in the Deep Atlantic Layer of Ice-Covered Amundsen Gulf (Beaufort Sea) in Winter." *Polar Biology* 34: 1959–1971.

Gjøsæter, H., M. Huserbråten, F. Vikebø, and E. Eriksen. 2020. "Key Processes Regulating the Early Life History of Barents Sea Polar Cod." *Polar Biology* 43: 1015–1027.

Gladish, C. V., D. M. Holland, A. Rosing-Asvid, J. W. Behrens, and J. Boje. 2015. "Oceanic Boundary Conditions for Jakobshavn Glacier. Part I: Variability and Renewal of Ilulissat Icefjord Waters, 2001–14." *Journal of Physical Oceanography* 45, no. 1: 3–32.

Gordeeva, N. V., and A. V. Mishin. 2019. "Population Genetic Diversity of Arctic Cod (*Boreogadus saida*) of Russian Arctic Seas." *Journal of Ichthyology* 59: 246–254.

Goudet, J. 2005. "Hierfstat, a Package for R to Compute and Test Hierarchical F-Statistics." *Molecular Ecology Notes* 5, no. 1: 184–186.

Graham, M., and H. Hop. 1995. "Aspects of Reproduction and Larval Biology of Arctic Cod (*Boreogadus saida*)." *Arctic* 48, no. 2: 130–135.

Hardy, S. M., C. M. Carr, M. Hardman, D. Steinke, E. Corstorphine, and C. Mah. 2011. "Biodiversity and Phylogeography of Arctic Marine Fauna: Insights From Molecular Tools." *Marine Biodiversity* 41: 195–210.

Hellberg, M. E. 2009. "Gene Flow and Isolation Among Populations of Marine Animals." *Annual Review of Ecology, Evolution, and Systematics* 40: 291–310.

Hempel, G., and K. Sherman. 2003. *Large Marine Ecosystems of the World: Trends in Exploitation, Protection, and Research*. Elsevier.

Hoff, S. N. K., M. Maurstad, O. K. Tørresen, et al. 2024. "Chromosomal Fusions and Large-Scale Inversions Are Key Features for Adaptation in Arctic Codfish Species." *bioRxiv*, Preprint. https://doi.org/10.1101/2024.06.28.599280.

Hoff, S. N. K., M. F. Maurstad, A. Le Moan, et al. 2024. "Population Divergence Manifested by Genomic Rearrangements in a Keystone Arctic Species With High Gene Flow." *bioRxiv*, Preprint. https://doi.org/10.1101/2024.06.28.597535.

Hu, X., P. G. Myers, and Y. Lu. 2019. "Pacific Water Pathway in the Arctic Ocean and Beaufort Gyre in Two Simulations With Different Horizontal Resolutions." *Journal of Geophysical Research: Oceans* 124, no. 8: 6414–6432.

Huang, Y., P. G. D. Feulner, C. Eizaguirre, et al. 2019. "Genome-Wide Genotype-Expression Relationships Reveal Both Copy Number and Single Nucleotide Differentiation Contribute to Differential Gene Expression Between Stickleback Ecotypes." *Genome Biology and Evolution* 11: 2344–2359.

Huserbråten, M. B. O., E. Eriksen, H. Gjøsæter, and F. Vikebø. 2019. "Polar Cod in Jeopardy Under the Retreating Arctic Sea Ice." *Communications Biology* 2, no. 1: 407.

ICES. 2013a. "Report of the Working Group on Improving Use of Survey Data for Assessment and Advice (WGISDAA), Dublin: Ireland." ICES Document CM 2013/SSGESST.

ICES. 2013b. "Report of the Workshop on Northeast Atlantic Mackerel Monitoring and Methodologies Including Science and Industry Involvement (WKNAMMM), Copenhagen and Hirtshals: Denmark." ICES Document CM 2013/SSGESST.

Jakobsson, M., L. A. Mayer, C. Bringensparr, et al. 2020. "The International Bathymetric Chart of the Arctic Ocean Version 4.0." *Scientific Data* 7, no. 1: 176.

Jakobsson, M., and N. A. Rosenberg. 2007. "CLUMPP: A Cluster Matching and Permutation Program for Dealing With Label Switching

and Multimodality in Analysis of Population Structure." *Bioinformatics* 23, no. 14: 1801–1806.

Johansen, T., F. Besnier, M. Quintela, et al. 2020. "Genomic Analysis Reveals Neutral and Adaptive Patterns That Challenge the Current Management Regime for East Atlantic Cod *Gadus morhua* L." *Evolutionary Applications* 13, no. 10: 2673–2688.

Jombart, T., and I. Ahmed. 2011. "Adegenet 1.3-1: New Tools for the Analysis of Genome-Wide SNP Data." *Bioinformatics* 27, no. 21: 21.

Jombart, T., S. Devillard, and F. Balloux. 2010. "Discriminant Analysis of Principal Components: A New Method for the Analysis of Genetically Structured Populations." *BMC Genetics* 11, no. 1: 1–15.

Jones, E. P., L. G. Anderson, and J. H. Swift. 1998. "Distribution of Atlantic and Pacific Waters in the Upper Arctic Ocean: Implications for Circulation." *Geophysical Research Letters* 25, no. 6: 765–768.

Jones, F. C., M. G. Grabherr, Y. F. Chan, et al. 2012. "The Genomic Basis of Adaptive Evolution in Threespine Sticklebacks." *Nature* 484: 55–61.

Kamvar, Z. N., J. F. Tabima, and N. J. Grünwald. 2014. "Poppr: An R Package for Genetic Analysis of Populations With Clonal, Partially Clonal, and/or Sexual Reproduction." *PeerJ* 2: e281.

Kessel, S. T., N. E. Hussey, R. E. Crawford, et al. 2017. "First Documented Large-Scale Horizontal Movements of Individual Arctic Cod (*Boreogadus saida*)." *Canadian Journal of Fisheries and Aquatic Sciences* 74, no. 3: 292–296.

Kim, Y.-H., S.-K. Min, N. P. Gillett, D. Notz, and E. Malinina. 2023. "Observationally-Constrained Projections of an Ice-Free Arctic Even Under a Low Emission Scenario." *Nature Communications* 14: 3139.

Kirubakaran, T. G., H. Grove, M. P. Kent, et al. 2016. "Two Adjacent Inversions Maintain Genomic Differentiation Between Migratory and Stationary Ecotypes of Atlantic Cod." *Molecular Ecology* 25, no. 10: 2130–2143.

Knutsen, H., P. E. Jorde, J. A. Hutchings, et al. 2018. "Stable Coexistence of Genetically Divergent Atlantic Cod Ecotypes at Multiple Spatial Scales." *Evolutionary Applications* 11, no. 9: 1527–1539.

Kohlbach, D., F. L. Schaafsma, M. Graeve, et al. 2017. "Strong Linkage of Polar Cod (*Boreogadus saida*) to Sea Ice Algae-Produced Carbon: Evidence From Stomach Content, Fatty Acid and Stable Isotope Analyses." *Progress in Oceanography* 152: 62–74.

Kono, Y., H. Sasaki, Y. Kurihara, A. Fujiwara, J. Yamamoto, and Y. Sakurai. 2016. "Distribution Pattern of Polar Cod (*Boreogadus saida*) Larvae and Larval Fish Assemblages in Relation to Oceanographic Parameters in the Northern Bering Sea and Chukchi Sea." *Polar Biology* 39: 1039–1048.

Korshunova, E. 2012. *Reproduction and Winter Biology of Polar Cod Boreogadus saida From Svalbard Waters*. Master thesis, Universitetet i Tromsø.

Krumpen, T., H. J. Belter, A. Boetius, et al. 2019. "Arctic Warming Interrupts the Transpolar Drift and Affects Long-Range Transport of Sea Ice and Ice-Rafted Matter." *Scientific Reports* 9, no. 1: 1.

Kumar, A., J. Yadav, and R. Mohan. 2020. "Global Warming Leading to Alarming Recession of the Arctic Sea-Ice Cover: Insights From Remote Sensing Observations and Model Reanalysis." *Heliyon* 6, no. 7: e04355.

Kwok, R., G. Spreen, and S. Pang. 2013. "Arctic Sea Ice Circulation and Drift Speed: Decadal Trends and Ocean Currents." *Journal of Geophysical Research: Oceans* 118, no. 5: 2408–2425.

Langmead, B., and S. L. Salzberg. 2012. "Fast Gapped-Read Alignment With Bowtie 2." *Nature Methods* 9, no. 4: 357–359.

Lannuzel, D., L. Tedesco, M. Van Leeuwe, et al. 2020. "The Future of Arctic Sea-Ice Biogeochemistry and Ice-Associated Ecosystems." *Nature Climate Change* 10, no. 11: 983–992.

Laurel, B. J., L. A. Copeman, M. Spencer, and P. Iseri. 2018. "Comparative Effects of Temperature on Rates of Development and Survival of Eggs and Yolk-Sac Larvae of Arctic Cod (*Boreogadus saida*) and Walleye Pollock (*Gadus chalcogrammus*)." *ICES Journal of Marine Science* 75, no. 7: 2403–2412.

Legendre, P., and E. D. Gallagher. 2001. "Ecologically Meaningful Transformations for Ordination of Species Data." *Oecologia* 129: 271–280.

Li, Y.-L., and J.-X. Liu. 2018. "Structure Selector: A Web-Based Software to Select and Visualize the Optimal Number of Clusters Using Multiple Methods." *Molecular Ecology Resources* 18: 176–177.

Lotterhos, K. E., and M. C. Whitlock. 2014. "Evaluation of Demographic History and Neutral Parameterization on the Performance of F_{ST} Outlier Tests." *Molecular Ecology* 23, no. 9: 2178–2192.

Luu, K., E. Bazin, and M. G. Blum. 2017. "Pcadapt: An R Package to Perform Genome Scans for Selection Based on Principal Component Analysis." *Molecular Ecology Resources* 17, no. 1: 67–77.

Madsen, M. L., R. J. Nelson, S.-E. Fevolden, J. S. Christiansen, and K. Præbel. 2016. "Population Genetic Analysis of Euro-Arctic Polar Cod *Boreogadus saida* Suggests Fjord and Oceanic Structuring." *Polar Biology* 39: 969–980.

Maes, S. M., H. Christiansen, F. C. Mark, et al. 2021. "High Gene Flow in Polar Cod (*Boreogadus saida*) From West-Svalbard and the Eurasian Basin." *Journal of Fish Biology* 99, no. 1: 49–60.

Maruki, T., and M. Lynch. 2017. "Genotype Calling From Population-Genomic Sequencing Data." *G3: Genes, Genomes, Genetics* 7, no. 5: 1393–1404.

Mathiesen, S. S., J. Thyrring, J. Hemmer-Hansen, et al. 2017. "Genetic Diversity and Connectivity Within *Mytilus* Spp. in the Subarctic and Arctic." *Evolutionary Applications* 10, no. 1: 39–55.

Melnikov, I. A., and N. V. Chernova. 2013. "Characteristics of Under-Ice Swarming of Polar Cod *Boreogadus saida* (Gadidae) in the Central Arctic Ocean." *Journal of Ichthyology* 53: 7–15.

Mérot, C. 2020. "Making the Most of Population Genomic Data to Understand the Importance of Chromosomal Inversions for Adaptation and Speciation." *Molecular Ecology* 29: 2513–2516.

Methot, R. D. 1986. "Frame Trawl for Sampling Pelagic Juvenile Fish." *CalCOFI Reports* 27: 267–278.

Miller, J. M., C. I. Cullingham, and R. M. Peery. 2020. "The Influence of a Priori Grouping on Inference of Genetic Clusters: Simulation Study and Literature Review of the DAPC Method." *Heredity* 125, no. 5: 269–280.

Møller, E. F., A. Christensen, J. Larsen, et al. 2023. "The Sensitivity of Primary Productivity in Disko Bay, a Coastal Arctic Ecosystem, to Changes in Freshwater Discharge and Sea Ice Cover." *Ocean Science* 19, no. 2: 403–420.

Moskalenko, B. F. 1964. "O Biologii Polyarnoi Treski (Saiki) *Boreogadus saida* (Lepechin). (On the Biology of Polar Cod *Boreogadus saida* (Lepechin))." *Voprosy Ichtiologii* 4: 433–443.

Mueter, F. J., J. Nahrgang, R. John Nelson, and J. Berge. 2016. "The Ecology of Gadid Fishes in the Circumpolar Arctic With a Special Emphasis on the Polar Cod (*Boreogadus saida*)." *Polar Biology* 39: 961–967.

Nelson, R. J., C. Bouchard, L. Fortier, et al. 2020. "Circumpolar Genetic Population Structure of Polar Cod, *Boreogadus saida*." *Polar Biology* 43: 951–961.

Nielsen, E. E., J. Hemmer-Hansen, P. F. Larsen, and D. Bekkevold. 2009. "Population Genomics of Marine Fishes: Identifying Adaptive Variation in Space and Time." *Molecular Ecology* 18, no. 15: 3128–3150. https://doi.org/10.1111/j.1365-294X.2009.04272.x.

Niiranen, S., A. Richter, T. Blenckner, L. C. Stige, M. Valman, and A.-M. Eikeset. 2018. "Global Connectivity and Cross-Scale Interactions

Create Uncertainty for Blue Growth of Arctic Fisheries." *Marine Policy* 87: 321–330.

Oksanen, J., R. Kindt, P. Legendre, et al. 2007. "The Vegan Package." *Community Ecology Package* 10, no. 631–637: 719.

Orlova, S. Y., A. A. Volkov, D. M. Shcepetov, et al. 2019. "Inter-and Intra-Species Relationships of Greenland Halibut *Reinhardtius hippoglossoides* (Pleuronectidae) Based on the Analysis of Nuclear and Mitochondrial Genetic Markers." *Journal of Ichthyology* 59: 65–77.

Pálsson, S., T. Källman, J. Paulsen, and E. Árnason. 2009. "An Assessment of Mitochondrial Variation in Arctic Gadoids." *Polar Biology* 32: 471–479.

Palumbi, S. R. 2003. "Population Genetics, Demographic Connectivity, and the Design of Marine Reserves." *Ecological Applications* 13, no. 1: S146–S158.

PAME. 2015. *Arctic Marine Strategic Plan. Protecting Marine and Coastal Ecosystems in a Changing Arctic*, 22. Arctic Council.

PAME, CAFF, S. Guðmundsdóttir, T. Barry, and H. Helgason. 2017. *Arctic Protected Areas; Indicator Report*. Arctic Council.

Pan, M., and H. P. Huntington. 2016. "A Precautionary Approach to Fisheries in the Central Arctic Ocean: Policy, Science, and China." *Marine Policy* 63: 153–157.

Pante, E., and B. Simon-Bouhet. 2013. "Marmap: A Package for Importing, Plotting and Analysing Bathymetric and Topographic Data in R." *PLoS One* 8, no. 9: e73051.

Paradis, E. 2010. "pegas: An R Package for Population Genetics With an Integrated–Modular Approach." *Bioinformatics* 26, no. 3: 419–420.

Pascual, M., B. Rives, C. Schunter, and E. Macpherson. 2017. "Impact of Life History Traits on Gene Flow: A Multispecies Systematic Review Across Oceanographic Barriers in the Mediterranean Sea." *PLoS One* 12, no. 5: e0176419. https://doi.org/10.1371/journal.pone.0176419.

Peng, G., and W. N. Meier. 2018. "Temporal and Regional Variability of Arctic Sea-Ice Coverage From Satellite Data." *Annals of Glaciology* 59, no. 76pt2: 191–200.

Pettitt-Wade, H., L. L. Loseto, A. Majewski, and N. E. Hussey. 2021. "Cod Movement Ecology in a Warming World: Circumpolar Arctic Gadids." *Fish and Fisheries* 22: 562–591.

Pfirman, S., W. F. Haxby, R. Colony, and I. Rigor. 2004. "Variability in Arctic Sea Ice Drift." *Geophysical Research Letters* 31, no. L16402: 1–4.

Pickart, R. S. 2004. "Shelfbreak Circulation in the Alaskan Beaufort Sea: Mean Structure and Variability." *Journal of Geophysical Research: Oceans* 109, no. C04024: 1–14.

Pineda, J., J. A. Hare, and S. Sponaugle. 2007. "Consequences for Population Connectivity." *Oceanography* 20, no. 3: 22–39.

Pinsky, M. L., and S. R. Palumbi. 2014. "Meta-Analysis Reveals Lower Genetic Diversity in Overfished Populations." *Molecular Ecology* 23, no. 1: 29–39.

Ponomarenko, V. P. 1968. "Some Data on the Distribution and Migrations of Polar Cod in the Seas of the Soviet Arctic." *Rapports et procès-verbaux des réunions du Conseil Permanent International pour l'Exploration de la Mer* 158: 131–135. https://doi.org/10.17895/ices.pub.19275398.

Ponomarenko, V. P. 2000. "Eggs, Larvae, and Juveniles of Polar Cod *Boreogadus saida* in the Barents, Kara, and White Seas." *Journal of Ichthyology* 40, no. 2: 165–173.

Præbel, K., J. I. Westgaard, S. E. Fevolden, and J. S. Christiansen. 2008. "Circumpolar Genetic Population Structure of Capelin *Mallotus villosus*." *Marine Ecology Progress Series* 360: 189–199.

Pritchard, J. K., M. Stephens, and P. Donnelly. 2000. "Inference of Population Structure Using Multilocus Genotype Data." *Genetics* 155, no. 2: 945–959.

Puechmaille, S. J. 2016. "The Program Structure Does Not Reliably Recover the Correct Population Structure When Sampling Is Uneven: Subsampling and New Estimators Alleviate the Problem." *Molecular Ecology Resources* 16: 608–627.

Quintela, M., S. Bhat, K. Præbel, et al. 2021. "Distinct Genetic Clustering in the Weakly Differentiated Polar Cod, *Boreogadus saida* Lepechin, 1774 From East Siberian Sea to Svalbard." *Polar Biology* 44, no. 8: 1711–1724.

Regan, H. C., C. Lique, and T. W. Armitage. 2019. "The Beaufort Gyre Extent, Shape, and Location Between 2003 and 2014 From Satellite Observations." *Journal of Geophysical Research: Oceans* 124, no. 2: 844–862.

Riginos, C., E. D. Crandall, L. Liggins, P. Bongaerts, and E. A. Treml. 2016. "Navigating the Currents of Seascape Genomics: How Spatial Analyses Can Augment Population Genomic Studies." *Current Zoology* 62, no. 6: 581–601.

Rochette, N. C., A. G. Rivera-Colón, and J. M. Catchen. 2019. "Stacks 2: Analytical Methods for Paired-End Sequencing Improve RADseq-Based Population Genomics." *Molecular Ecology* 28, no. 21: 4737–4754.

Roy, D., D. C. Hardie, M. A. Treble, J. D. Reist, and D. E. Ruzzante. 2014. "Evidence Supporting Panmixia in Greenland Halibut (*Reinhardtius hippoglossoides*) in the Northwest Atlantic." *Canadian Journal of Fisheries and Aquatic Sciences* 71, no. 5: 763–774.

Rysgaard, S., W. Boone, D. Carlson, et al. 2020. "An Updated View on Water Masses on the Pan-West Greenland Continental Shelf and Their Link to Proglacial Fjords." *Journal of Geophysical Research: Oceans* 125, no. 2: e2019JC015564.

Saha, A., T. Johansen, R. Hedeholm, et al. 2017. "Geographic Extent of Introgression in *Sebastes mentella* and Its Effect on Genetic Population Structure." *Evolutionary Applications* 10, no. 1: 77–90.

Schaafsma, F. L., H. Flores, C. L. David, et al. 2024. "Insights Into the Diet and Feeding Behaviour of Immature Polar Cod (*Boreogadus saida*) From the Under-Ice Habitat of the Central Arctic Ocean." *Journal of Fish Biology* 105: 907–930.

Schiebelhut, L. M., and M. N. Dawson. 2018. "Correlates of Population Genetic Differentiation in Marine and Terrestrial Environments." *Journal of Biogeography* 45, no. 11: 2427–2441. https://doi.org/10.1111/jbi.13437.

Sherman, K., M. Sissenwine, V. Christensen, et al. 2005. "A Global Movement Toward an Ecosystem Approach to Management of Marine Resources." *Marine Ecology Progress Series* 300: 275–279.

Silliman, K., and D. Davenport. 2022. "Radseq. MarineOmics." https://marineomics.github.io/RADseq.html.

Siron, R., K. Sherman, H. R. Skjoldal, and E. Hiltz. 2008. "Ecosystem-Based Management in the Arctic Ocean: A Multi-Level Spatial Approach." *Arctic* 61, no. Suppl. 1: 86–102.

Snoeijs-Leijonmalm, P., H. Gjøsæter, R. B. Ingvaldsen, et al. 2021. "A Deep Scattering Layer Under the North Pole Pack Ice." *Progress in Oceanography* 194: 102560.

Sodeland, M., P. E. Jorde, S. Lien, et al. 2016. "'Islands of Divergence' in the Atlantic Cod Genome Represent Polymorphic Chromosomal Rearrangements." *Genome Biology and Evolution* 8: 1012–1022.

Spalding, M. D., H. E. Fox, G. R. Allen, et al. 2007. "Marine Ecoregions of the World: A Bioregionalization of Coastal and Shelf Areas." *Bioscience* 57, no. 7: 573–583.

Spencer, M. L., C. D. Vestfals, F. J. Mueter, and B. J. Laurel. 2020. "Ontogenetic Changes in the Buoyancy and Salinity Tolerance of Eggs and Larvae of Polar Cod (*Boreogadus saida*) and Other Gadids." *Polar Biology* 43: 1141–1158.

Spreen, G., S. Kern, D. Stammer, and E. Hansen. 2009. "Fram Strait Sea Ice Volume Export Estimated Between 2003 and 2008 From Satellite Data." *Geophysical Research Letters* 36, no. 19: 1–6.

Steiner, N. S., J. Bowman, K. Campbell, et al. 2021. "Climate Change Impacts on Sea-Ice Ecosystems and Associated Ecosystem Services." *Elementa: Science of the Anthropocene* 9, no. 1: 7.

Stinchcombe, J. R., and H. E. Hoekstra. 2008. "Combining Population Genomics and Quantitative Genetics: Finding the Genes Underlying Ecologically Important Traits." *Heredity* 100, no. 2: 158–170. https://doi.org/10.1038/sj.hdy.6800937.

Thomas, D. N., D. L. Arévalo-Martínez, K. C. Crocket, et al. 2022. "A Changing Arctic Ocean." *Ambio* 51, no. 2: 293–297.

Thomson, J., Y. Fan, S. Stammerjohn, et al. 2016. "Emerging Trends in the Sea State of the Beaufort and Chukchi Seas." *Ocean Modelling* 105: 1–12.

Vestfals, C. D., F. J. Mueter, K. S. Hedstrom, et al. 2021. "Modeling the Dispersal of Polar Cod (*Boreogadus saida*) and Saffron Cod (*Eleginus gracilis*) Early Life Stages in the Pacific Arctic Using a Biophysical Transport Model." *Progress in Oceanography* 196: 102571.

Vihtakari, M., B. Þ. Elvarsson, M. Treble, et al. 2022. "Migration Patterns of Greenland Halibut in the North Atlantic Revealed by a Compiled Mark–Recapture Dataset." *ICES Journal of Marine Science* 79, no. 6: 1902–1917.

Vis, M. L., S. M. Carr, W. R. Bowering, and W. S. Davidson. 1997. "Greenland Halibut (*Reinhardtius hippoglossoides*) in the North Atlantic Are Genetically Homogeneous." *Canadian Journal of Fisheries and Aquatic Sciences* 54, no. 8: 1813–1821.

Wassmann, P. 2011. "Arctic Marine Ecosystems in an Era of Rapid Climate Change." *Progress in Oceanography* 90, no. 1–4: 1–17.

Weir, B. S., and C. C. Cockerham. 1984. "Estimating F-Statistics for the Analysis of Population Structure." *Evolution* 38: 1358–1370.

Welch, H. E., M. A. Bergmann, T. D. Siferd, et al. 1992. "Energy Flow Through the Marine Ecosystem of the Lancaster Sound Region, Arctic Canada." *Arctic* 45, no. 4: 343–357.

Westgaard, J.-I., A. Saha, M. Kent, et al. 2017. "Genetic Population Structure in Greenland Halibut (*Reinhardtius hippoglossoides*) and Its Relevance to Fishery Management." *Canadian Journal of Fisheries and Aquatic Sciences* 74, no. 4: 475–485.

Whitlock, M. C., and K. E. Lotterhos. 2015. "Reliable Detection of Loci Responsible for Local Adaptation: Inference of a Null Model Through Trimming the Distribution of F_{ST}." *American Naturalist* 186, no. S1: S24–S36.

Wildes, S. L., J. Whittle, H. Nguyen, and J. Guyon. 2016. *Boreogadus saida Genetics in the Alaskan Arctic (OCS Study BOEM 2011-AK-11-08 a/b).* US Department of the Interior, Bureau of Ocean Energy Management.

Wilson, R. E., G. K. Sage, K. Wedemeyer, et al. 2019. "Micro-Geographic Population Genetic Structure Within Arctic Cod (*Boreogadus saida*) in Beaufort Sea of Alaska." *ICES Journal of Marine Science* 76, no. 6: 1713–1721.

Wilson, R. E., S. A. Sonsthagen, N. Smé, et al. 2020. "Mitochondrial Genome Diversity and Population Mitogenomics of Polar Cod (*Boreogadus saida*) and Arctic Dwelling Gadoids." *Polar Biology* 43: 979–994.

Winsor, P., and D. C. Chapman. 2004. "Pathways of Pacific Water Across the Chukchi Sea: A Numerical Model Study." *Journal of Geophysical Research: Oceans* 109, no. C03002: 1–16.

Wood, K. R., N. A. Bond, S. L. Danielson, et al. 2015. "A Decade of Environmental Change in the Pacific Arctic Region." *Progress in Oceanography* 136: 12–31.

Yeomans, K. A., and P. A. Golder. 1982. "The Guttman-Kaiser Criterion as a Predictor of the Number of Common Factors." *Statistician* 31: 221–229.

Zheng, X., D. Levine, J. Shen, S. M. Gogarten, C. Laurie, and B. S. Weir. 2012. "A High-Performance Computing Toolset for Relatedness and Principal Component Analysis of SNP Data." *Bioinformatics* 28, no. 24: 3326–3328.

Supporting Information

Additional supporting information can be found online in the Supporting Information section.